

# Steady states of the parametric rotator and pendulum

Antonio O. Bouzas \*

Departamento de Física Aplicada, CINVESTAV-IPN  
Carretera Antigua a Progreso Km. 6, Apdo. Postal 73 “Cordemex”  
Mérida 97310, Yucatán, México

## Abstract

We discuss several steady-state rotation and oscillation modes of the planar parametric rotator and pendulum with damping. We consider a general elliptic trajectory of the suspension point for both rotator and pendulum, for the latter at an arbitrary angle with gravity, with linear and circular trajectories as particular cases. We treat the damped, non-linear equation of motion of the parametric rotator and pendulum perturbatively for small parametric excitation and damping, although our perturbative approach can be extended to other regimes as well. Our treatment involves only ordinary second-order differential equations with constant coefficients, and provides numerically accurate perturbative solutions in terms of elementary functions. Some of the steady-state rotation and oscillation modes studied here have not been discussed in the previous literature. Other well-known ones, such as parametric resonance and the inverted pendulum, are extended to elliptic parametric excitation tilted with respect to gravity. The results presented here should be accessible to advanced undergraduates, and of interest to graduate students and specialists in the field of non-linear mechanics.

## 1 Introduction

A physical system is said to be parametrically excited when some of its parameters vary periodically with time. One of the simplest examples of a parametrically excited system consists of a rigid rotator (or, in the presence of gravity, a physical pendulum) whose suspension point follows a periodic trajectory, with both rotator and suspension point restricted to move on a plane. The basic modes of motion of that system are rotation and oscillation. Depending on the type of parametric excitation, its amplitude, and the strength of damping, many different types of rotation and oscillation modes may be encountered in its spectrum of steady states. Furthermore, those basic modes combine to form complex motions in which rotation and oscillation alternate in regular or irregular patterns, including chaotic motion. A qualitative description of a variety of different modes of motion in a parametric pendulum, and some further references, is given in the introduction of [1].

The parametric rotator does not seem to have received much attention in the literature, despite the fact that its rich non-linear dynamics (see, for example, [2]) is interesting for both research and education purposes. The parametric pendulum is discussed in the literature in relation to its two most remarkable dynamical phenomena. One of them is parametric resonance, that occurs in systems possessing normal modes of oscillation when the period of the parametric excitation is an integer or half-integer multiple of the period of a normal mode. Parametric resonance in a pendulum with vertically or horizontally moving suspension point is discussed in the textbooks [3, 4], and in [5–8]. Parametric resonance has also been discussed in the context of the elastic or spring pendulum [9–12], a linear oscillator [13, 14], elastic strings [10, 15], electronic circuits [10, 16], and many other systems.

The other striking dynamical aspect of the parametric pendulum is the so-called “inverted pendulum.” A vertical parametric excitation, with sufficiently large amplitude and frequency, causes the upright, usually unstable, equilibrium position of the pendulum to become stable. The dynamical stabilisation involved in this phenomenon is of interest by itself, and also because it constitutes a mechanical analogy for similar mechanisms in more complex systems [17, 18]. A detailed study of the inverted pendulum was given by Kapitza [19]. Textbook treatments are given in [20, 21]. In the more recent literature a significant number of

---

\*E-mail: abouzas@fis.mda.cinvestav.mx

studies of the inverted pendulum exist, both experimental [18,22–24] and theoretical [1,2,5,17,21,25–32] (see also the references cited in those papers). Most of those theoretical works deal with the non-linear equation of motion of the parametric pendulum by linearising it in the small-oscillation approximation [21,25,26,29,31] in which it reduces to a Mathieu equation (see, e.g., [33] and references therein), or within the framework of the effective potential by separation of slow and fast variables [1,2,20], or by considering non-sinusoidal motion of the suspension point [5,27,28]. In most cases damping is justifiably neglected. All of those theoretical approaches lead to important insights into the dynamics of the inverted pendulum, and to quantitative results such as, for example, the determination of its region of stability.

In this paper we adopt a complementary point of view. We look for steady-state solutions to the damped, non-linear equation of motion of the parametric rotator and pendulum. Our approach is based on the observation that the basic steady-state rotation and oscillation modes are mathematically simple, in the sense that they can be expressed in terms of elementary functions in some perturbative expansion. For such basic modes the non-linearity of the equation of motion manifests itself in the multiplicity of different regimes, characterised by a few dimensionless parameters, leading to different types of solution and requiring different perturbative expansions. Here, we restrict ourselves to small parametric excitations and low to moderate damping (both to be quantified below), and set up a perturbative expansion in the small excitation amplitude. In that regime the spectrum of basic modes of motion is simpler than at larger amplitudes, though still complex, but more interesting than in the limit of high friction. The cases of large parametric excitations and/or large friction could, in principle, be handled by straightforward modifications of our perturbative method. Some of the steady-state rotation and oscillation modes studied here have not been discussed in the previous literature. Other well-known ones, such as parametric resonance and the inverted pendulum, are extended to elliptic parametric excitation tilted with respect to gravity.

A pedagogical advantage of the approach adopted here is that it yields numerically accurate approximate solutions to the equations of motion of realistic non-linear systems like the parametric rotator and pendulum by elementary mathematical methods. The only technical requirements are the ability to perform power-series expansions and to solve inhomogeneous ordinary second-order differential equations with constant coefficients, which should be familiar from a course on analytical mechanics. Thus, we hope that the analysis in the following sections may contribute to our understanding of non-linear mechanics, and to make the latter more widely accessible to both students and educators.

The paper is organised as follows. In the next section we derive the equation of motion for the rotator with general elliptic motion of its suspension point, subject to gravity and damping, and establish our notation and conventions. In section 3 we discuss the two-dimensional rotator with small linear parametric excitation, in the absence of gravity, explaining in detail the perturbative method to solve the equation of motion for the steady-state of the system. The same perturbative approach is applied in the subsequent sections. The extension of the results of section 3 to general elliptic parametric excitation is carried out in section 4. The inclusion of gravity is considered in section 5, where we study rotation and oscillation modes of the parametric pendulum elliptically excited at an arbitrary angle with gravity. Steady states related to parametric resonance are discussed separately in section 6. Finally, in section 7 we give our summary and final remarks.

## 2 The parametric rotator

We consider a two-dimensional rotator, that is, a rigid body free to rotate about one of its points whose trajectory in space is fixed. We call the rotator symmetric if its suspension point is at its centre of mass, otherwise asymmetric. If a rotator is symmetric, a spatially constant force field, such as an inertial or gravitational force, cannot exert a torque on it. To be specific, we will think of a thin homogeneous bar of mass  $M$  and length  $L$  with its suspension point at a distance  $L_1$  from one of its ends and  $L_2$  from the other ( $L_1 + L_2 = L$ ,  $L_1 > L_2$ ). If we denote by  $\vec{r}_0$  the position of the suspension point, and by  $\xi$  a coordinate along the bar,  $-L_2 \leq \xi \leq L_1$ , the points on the bar are parameterised by  $\vec{r}(\xi, t) = \xi \sin \theta \hat{x} - \xi \cos \theta \hat{z} + \vec{r}_0$ .

It will be convenient to choose a coordinate system such that the gravitational force points not in the

direction  $-\hat{z}$ , but forming an angle  $-\alpha$  with it. The rotator's Lagrangian is then, up to total derivatives,

$$\begin{aligned} \mathbf{L} &= \frac{1}{2} \int_{-L_2}^{L_1} d\xi \frac{M}{L} \dot{\vec{r}}(\xi, t)^2 - \int_{-L_2}^{L_1} d\xi \frac{M}{L} g(\cos \alpha z_0 - \cos \alpha \cos \theta \xi + \sin \alpha x_0 + \sin \alpha \sin \theta \xi) \\ &= \frac{1}{2} \mathcal{I} \dot{\theta}^2 + \frac{1}{2} M(L_1 - L_2) (\sin \theta \dot{x}_0 - \cos \theta \dot{z}_0) + \frac{1}{2} M \dot{r}_0^2 + \frac{1}{2} M g(L_1 - L_2) \cos(\theta + \alpha) \\ &\quad - M g(\cos \alpha z_0 + \sin \alpha x_0) , \end{aligned} \quad (1)$$

where  $\mathcal{I} = M/3(L_1^2 + L_2^2 - L_1 L_2)$  is the moment of inertia with respect to the suspension point, and where in the second equality we dropped a total derivative. In what follows we always take into account the effect on the rotator of friction, in the form of viscous damping proportional to its angular velocity. Adding such term to the equation of motion for  $\theta$  from the Lagrangian (1) we obtain

$$\mathcal{I}(\ddot{\theta} + \lambda \dot{\theta}) = \frac{1}{2} M(L_1 - L_2) (\cos \theta \dot{x}_0 + \sin \theta \dot{z}_0) - \frac{1}{2} M g(L_1 - L_2) \sin(\theta + \alpha) , \quad (2)$$

$\lambda$  being the damping coefficient. On the left-hand side of (2) the first term corresponds to the rotator's inertia and the second one to damping due to friction. On the right-hand side, the first term describes the torque applied on the rotator by the inertial forces due to the accelerated motion of its suspension point, and the second one the torque due to gravity. Notice that the right-hand side vanishes for a symmetric rotator.

We restrict ourselves to the case where the suspension point traces an elliptic trajectory about the origin with a single frequency  $\gamma$ ,

$$x_0(t) = -r_0 \sin \epsilon \sin(\gamma t) , \quad z_0(t) = r_0 \cos(\gamma t) , \quad (3)$$

with  $r_0$  the length of its semi-major axis,  $r_0 \sin \epsilon$  that of its semi-minor axis. Notice that we have chosen the  $z$  axis along the major axis of the ellipse (3), which explains why we took gravity along an arbitrary direction in (1). Substituting (3) in (2) we obtain the equation of motion for the rotator with an oscillating suspension point. It is convenient, however, to change the time variable in (2) to dimensionless time  $\tau = \gamma t$ , so as to express the equation in terms of a minimal set of dimensionless parameters. After doing so, we obtain,

$$\frac{d^2 \theta}{d\tau^2} + \tilde{\lambda} \frac{d\theta}{d\tau} + \Delta \frac{x_0(\tau)}{r_0} \cos \theta + \Delta \frac{z_0(\tau)}{r_0} \sin \theta + \Gamma \sin(\theta + \alpha) = 0 , \quad (4)$$

with  $\tilde{\lambda} = \lambda/\gamma$  the dimensionless damping coefficient and

$$\Delta = \frac{M(L_1^2 - L_2^2)}{2\mathcal{I}} \frac{r_0}{L} , \quad \Gamma = \frac{M(L_1^2 - L_2^2)}{2\mathcal{I}} \frac{g}{L\gamma^2} . \quad (5)$$

Equation (4) is generally valid for any rotator with its suspension point oscillating as in (3), and coefficients  $\Delta$ ,  $\Gamma$  depending on its geometry and mass distribution. For a symmetric rotator  $\Delta = 0 = \Gamma$ . For the homogeneous thin bar discussed above,  $\Delta$  and  $\Gamma$  are given by (5).

### 3 Linearly excited parametric rotator

We consider first the case in which the plane of the rotator is horizontal, so that gravity does not play a role ( $\Gamma = 0$  in (4)), and the motion of its suspension point is linear ( $\epsilon = 0$  in (3)). The equation of motion (4) then takes the form

$$\frac{d^2 \theta}{d\tau^2} + \tilde{\lambda} \frac{d\theta}{d\tau} + \frac{\Delta}{2} \sin(\theta + \tau) + \frac{\Delta}{2} \sin(\theta - \tau) = 0 . \quad (6)$$

Notice that in (6) we can always choose the time origin so that  $\Delta > 0$ , and that the equation is invariant under  $\theta \rightarrow -\theta$ . We restrict ourselves to the regime of small parametric excitations  $0 < \Delta \lesssim 1$ .

#### 3.1 Basic solution

We look for steady-state solutions to (6) with  $\theta(\tau)$  linearly rising with  $\tau$ , and possibly performing small oscillations about that linear trajectory. Thus, we are led to propose a solution of the form

$$\theta(\tau) = \omega \tau + \Theta_0 + f(\tau) \Delta , \quad \omega \neq 0 , \quad (7)$$

with  $\Theta_0$  a constant phase. It is physically reasonable to include such constant term in  $\theta(\tau)$  because, due to the motion of the suspension point, the  $z$  axis is a privileged direction in space, making (6) sensitive to the phase of  $\theta$ . For instance,  $\theta = n\pi$  with integer  $n$  are equilibrium solutions to (6), but any other constant is not. The last term in (7) represents small oscillations with an amplitude of  $\mathcal{O}(\Delta)$ , which requires the unknown function  $f(\tau)$  to be bounded for  $0 \leq \tau < \infty$ .

If we substitute (7) in (6) and let  $\Delta \rightarrow 0$ , we find that  $\omega\tilde{\lambda} \rightarrow 0$ . We must therefore assume that  $\tilde{\lambda} = \mathcal{O}(\Delta)$ , which expresses the physically reasonable condition that, for small parametric excitations to cause steady-state rotations, friction must be correspondingly small. (The relation between  $\tilde{\lambda}$  and  $\Delta$  is made precise below in equation (11).) Thus, substituting (7) in (6) and neglecting terms of  $\mathcal{O}(\Delta^2)$  yields

$$\begin{aligned} \frac{d^2 f}{d\tau^2} = & -\omega \frac{\tilde{\lambda}}{\Delta} - \frac{1}{2} \sin((\omega + 1)\tau) \cos \Theta_0 - \frac{1}{2} \cos((\omega + 1)\tau) \sin \Theta_0 \\ & - \frac{1}{2} \sin((\omega - 1)\tau) \cos \Theta_0 - \frac{1}{2} \cos((\omega - 1)\tau) \sin \Theta_0 , \end{aligned} \quad (8)$$

where  $\tilde{\lambda}/\Delta$  remains finite as  $\Delta \rightarrow 0$ . Equation (8) is inconsistent with our assumptions, since the constant term on its right-hand side leads to an unbounded perturbation  $f(\tau) = -1/2(\omega\tilde{\lambda}/\Delta)\tau^2 + \dots$ , growing quadratically with  $\tau$ . The only way around this inconsistency is to set  $\omega = \pm 1$ , to obtain,

$$\frac{d^2 f}{d\tau^2} = \mp \frac{\tilde{\lambda}}{\Delta} - \frac{1}{2} \sin(\Theta_0) \mp \frac{1}{2} \sin(2\tau \pm \Theta_0) , \quad \omega = \pm 1 . \quad (9)$$

Setting now  $\sin(\Theta_0) = \mp 2\tilde{\lambda}/\Delta$ , the  $\tau$ -independent terms on the right-hand side of (9) vanish, and the equation admits a bounded solution  $f(\tau)$ . We have then a solution to (6) of the form  $\theta(\tau) = \pm\theta_0(\tau) + \mathcal{O}(\Delta)$  with,

$$\theta_0(\tau) = \tau + \Theta_0 , \quad \Theta_0 = -\arcsin(2\tilde{\lambda}/\Delta) + 2n\pi . \quad (10)$$

This result shows that for small  $\Delta$  there cannot be parametrically excited steady-state rotations unless

$$\tilde{\lambda} \leq \Delta/2 . \quad (11)$$

We notice also that the steady-state phase  $\Theta_0$  is completely determined by the non-linear dynamics and the damping, without reference to the initial conditions which, for times  $\tau \gg 1/\tilde{\lambda}$ , are completely erased by the damping interactions. We conclude that, in physical units of time, at small  $\Delta$  and  $\tilde{\lambda}$  satisfying (11), steady-state rotations occur only with the same angular frequency  $\gamma$  as the parametric excitation,  $\theta(t) = \pm(\gamma t + \Theta_0) + \mathcal{O}(\Delta)$ , either clockwise or counter-clockwise.

### 3.2 Perturbation theory: steady-state rotation

We now develop the considerations of the previous section into a systematic perturbative approach. We assume a solution to (6) of the form,

$$\theta(\tau) = \theta_0(\tau) + \sum_{n=1}^{\infty} \frac{\Delta^n}{n!} (f_n(\tau) + \Theta_n) , \quad (12)$$

with  $\theta_0(\tau)$  given by (10). We consider only positive-frequency solutions  $\theta(\tau)$  since, as noticed above, negative-frequency ones are just given by  $-\theta(\tau)$ . The perturbations  $f_n(\tau)$  in (12) are assumed to be bounded in  $0 \leq \tau < \infty$ , uniformly with respect to  $n$ . We have explicitly separated from  $f_n$  a constant term  $\Theta_n$ , so we further require that  $f_n(\tau)$  must not contain constant terms. The constants  $\Theta_n$  are perturbative corrections to the zeroth-order phase  $\Theta_0$  in (10).

Replacing (12) in (6) and expanding to first order in  $\Delta$  leads to equation (9) (with upper signs). With  $\Theta_0$  given by (10), and the condition that  $f_1(\tau)$  must not contain constant terms, we get a unique solution to (9)

$$f_1(\tau) = \frac{1}{8} \sin(2\tau + \Theta_0) . \quad (13)$$

In order to have a complete first-order solution we still need to find the constant  $\Theta_1$ , which is fixed by requiring consistency of the second-order equation.

To second order in  $\Delta$  equation (6) yields,

$$\frac{1}{2}\Delta^2 \frac{d^2 f_2}{d\tau^2} + \tilde{\lambda}\Delta \frac{df_1}{d\tau} + \frac{1}{2}\Delta^2 \cos(2\tau + \Theta_0)(f_1(\tau) + \Theta_1) + \frac{1}{2}\Delta^2 \cos(\Theta_0)(f_1(\tau) + \Theta_1) = 0 .$$

Substituting  $f_1$  in this equation we get, after some rearrangements,

$$\frac{d^2 f_2}{d\tau^2} = \cos(\Theta_0)\Theta_1 - \frac{3}{16} \sin(2\tau) + \frac{1}{16} \sin(2\tau + 2\Theta_0) - \frac{1}{16} \sin(4\tau + 2\Theta_0) . \quad (14)$$

The first term on the right-hand side is a constant that must vanish for  $f_2$  to be bounded, therefore

$$\Theta_1 = 0 . \quad (15)$$

We can now find  $f_2$  by twice integrating (14) with respect to  $\tau$ . The requirement that  $f_2$  should not contain zero-frequency terms leads to a unique solution,

$$f_2(\tau) = \frac{1}{2^8} \sin(4\tau + 2\Theta_0) + \frac{3}{2^6} \sin(2\tau) - \frac{1}{2^6} \sin(2\tau + 2\Theta_0) . \quad (16)$$

With this result the solution to (6) to  $\mathcal{O}(\Delta^2)$  is determined up to the constant  $\Theta_2$ , which results from requiring consistency of the third-order equation.

We proceed further to consider the terms of  $\mathcal{O}(\Delta^3)$  in equation (6) with (12). After substituting  $f_1$  and  $f_2$  in the third-order equation, somewhat lengthy algebra yields

$$\begin{aligned} \frac{d^2 f_3}{d\tau^2} = & \left( -\frac{3}{2} \cos(\Theta_0)\Theta_2 + \frac{15}{2^8} \sin(\Theta_0) \right) - \frac{3}{2} \cos(2\tau + \Theta_0)\Theta_2 - \frac{27}{2^8} \sin(2\tau - \Theta_0) + \frac{87}{2^{10}} \sin(2\tau + \Theta_0) \\ & - \frac{3}{2^8} \sin(2\tau + 3\Theta_0) - \frac{45}{2^{10}} \sin(4\tau + \Theta_0) + \frac{15}{2^{10}} \sin(4\tau + 3\Theta_0) - \frac{9}{2^{10}} \sin(6\tau + 3\Theta_0) . \end{aligned} \quad (17)$$

As before, boundedness of  $f_3$  means that the constant term in brackets must vanish, so that,

$$\Theta_2 = \frac{5}{2^7} \tan(\Theta_0) . \quad (18)$$

Now equation (17) can be integrated, taking into account that  $f_3(\tau)$  must not contain constant terms, to yield,

$$\begin{aligned} f_3(\tau) = & \frac{3}{8}\Theta_2 \cos(2\tau + \Theta_0) + \frac{27}{2^{10}} \sin(2\tau - \Theta_0) - \frac{87}{2^{12}} \sin(2\tau + \Theta_0) + \frac{3}{2^{10}} \sin(2\tau + 3\Theta_0) \\ & + \frac{45}{2^{14}} \sin(4\tau + \Theta_0) - \frac{15}{2^{14}} \sin(4\tau + 3\Theta_0) + \frac{1}{2^{12}} \sin(6\tau + 3\Theta_0) . \end{aligned} \quad (19)$$

The third-order correction is completed with the equality

$$\Theta_3 = \frac{15}{2^9} \sin(\Theta_0) , \quad (20)$$

required for consistency of the fourth-order equation.

The above results constitute a perturbative solution to (6) as a series expansion in  $\Delta$ , valid in the regime  $0 < \Delta \lesssim 1$  and when the condition (11) holds. The zeroth-order solution is (10). The first, second and third order solutions are given by,

$$\theta_1(\tau) = \theta_0(\tau) + f_1(\tau)\Delta , \quad \theta_2(\tau) = \theta_1(\tau) + (\Theta_2 + f_2(\tau))\frac{\Delta^2}{2} , \quad \theta_3(\tau) = \theta_2(\tau) + (\Theta_3 + f_3(\tau))\frac{\Delta^3}{6} . \quad (21)$$

Several remarks about this perturbative solution are in order. (a) In the perturbative expansion (12) we could have included corrections to the angular frequency, with a first term in (12) of the form  $(1 + \omega_1\Delta + \omega_2\Delta^2/2 + \dots)\tau$  instead of just  $\tau$ . All the corrections  $\omega_n$ , however, turn out to vanish. (b) The results (13), (16), (19), for  $f_{1,2,3}$  suggest that the perturbative expansion parameter is actually  $\Delta/8$  rather than  $\Delta$ , so the domain of applicability of perturbation theory should be larger than expected. This is confirmed below in section 3.5 on numerical results. (c)  $\Theta_0$  is determined only up to  $2n\pi$ . The additional  $n$  turns typically build up during the transient state. Our perturbative solutions hold valid only for times  $\tau \gg 1/\tilde{\lambda}$  after all transients have died off, and depend on  $\tilde{\lambda}$  only through the phase  $\Theta_0$ . (d) The perturbations  $f_n(\tau)$  contain only even frequencies (in physical units, only even multiples of  $\gamma$ ). Thus,  $\theta(\tau) - \tau$  is periodic with period  $\pi$ .

These results are numerically verified below in section 3.5, where they are compared with numerical solutions of (6) and found to be in tight agreement with them, each order significantly improving on the previous one. Those verifications justify our perturbative procedure, together with the implicit hypothesis that the dependence of  $\theta(\tau)$  on  $\Delta$  is analytic at  $\Delta = 0$ .

### 3.3 Steady-state oscillations

When condition (11) is not satisfied the steady-state rotation described in the previous section does not exist. In that case, the rotator may reach the equilibrium solutions  $\theta = n\pi$ . There is another type of steady-state solution that is possible in that case, however, describing oscillations about  $(2n + 1)\pi/2$ . To obtain those solutions we assume they have the form,

$$\theta(\tau) = \Theta_0 + \sum_{n=1}^{\infty} \frac{\Delta^n}{n!} (f_n(\tau) + \Theta_n) . \quad (22)$$

Substituting this form into the equation of motion (6) leads to perturbative equations for  $f_n$  that can be solved by the same method as in section 3.2. We will omit the details of the procedure for brevity, commenting only on the form of the solution.

The condition that the perturbation  $f_2(\tau)$  be bounded leads to  $\sin(2\Theta_0) = 0$ , whereas the equations at third, fourth and fifth order yield  $\Theta_1 = \Theta_2 = \Theta_3 = 0$ . If we set  $\Theta_0 = k\pi$ , for some integer  $k$ , we recover the equilibrium solutions and all corrections  $\Theta_n, f_n$  must vanish because  $\Theta_0$  is itself an exact solution to the equation of motion. Another possible choice is  $\Theta_0 = (2k + 1)\pi/2$ , with  $k$  an integer. In that case the solution is non trivial. At first order we obtain,

$$\theta_1(\tau) = \Theta_0 + \Delta \sin(\Theta_0) \cos(\tau) . \quad (23)$$

The equation for  $f_2$  yields the second-order solution,

$$\theta_2(\tau) = \theta_1(\tau) - \Delta \tilde{\lambda} \sin(\Theta_0) \sin(\tau) , \quad (24)$$

and at third order we find

$$\theta_3(\tau) = \theta_2(\tau) - \sin(\Theta_0) \left( \frac{9}{24} \Delta^3 \cos(\tau) + \Delta \tilde{\lambda}^2 \cos(\tau) + \frac{1}{72} \Delta^3 \cos(3\tau) \right) . \quad (25)$$

The perturbative method does not yield information on the domain of validity of these solutions in parameter space. Numerical analysis of (6) suggests that, in the perturbative regime  $\Delta, \tilde{\lambda} \lesssim 1$ , the steady state described by (23)–(25) exists only for  $\Delta \ll \tilde{\lambda}$ .

### 3.4 Order-of-magnitude estimates

The quantitative meaning of the parameter  $\Delta$  in (6) is apparent from its definition (5) for a homogeneous thin bar, or its correspondingly modified expressions for other rigid bodies. Thus, for example, for a homogeneous thin bar with  $L_1 = 5.4$  cm,  $L_2 = 4.6$  cm and excitation amplitude  $r_0 = 0.5$  cm we have  $\Delta = 0.016$ . For a larger, more asymmetric thin bar with  $L_1 = 13$  cm,  $L_2 = 7$  cm and amplitude  $r_0 = 2$  cm we obtain  $\Delta = 0.094 \simeq 0.1$ . By reducing the asymmetry or the amplitude we can get values of  $\Delta$  smaller by several orders of magnitude. With larger asymmetries and amplitudes  $\Delta$  can be made larger,  $\Delta \gtrsim 1$ . For values  $\Delta > 2$  the parametric-excitation amplitude must be larger than the length of the rotator itself, so rather than parametrically excited, the rotator should in that case more properly be referred to as orbitally excited.

In order to obtain some quantitative understanding of the parameter  $\tilde{\lambda}$  in (6), we consider the steady-state rotations described in section 3.2. Once the steady state has been reached, we may cease the parametric excitation and find out how many turns the rotator completes before it stops moving. Since for a steady-state rotation of the form (12) the (dimensionless) angular velocity is  $1 + \mathcal{O}(\Delta)$ , the number of turns sought for must be approximately  $1/(2\pi\tilde{\lambda})$  independently of  $\Delta$ . Indeed, after the motion of the suspension point has stopped, we find by numerically solving (6) with  $\Delta = 0$  that the rotator performs slightly more than 15 turns if  $\tilde{\lambda} = 10^{-2}$ , about 150 turns if  $\tilde{\lambda} = 10^{-3}$ , and about 1500 turns for  $\tilde{\lambda} = 10^{-4}$ . From our everyday experience we know that the first case corresponds to the level of damping usually encountered in common household appliances such as fans or mixers. The second case corresponds to a much lower level of damping, found in more special mechanical devices such as some microprocessor fans. In all three cases we find that the perturbative results of section 3.2 for the steady state agree with exact numerical solutions to (6) with high accuracy, as discussed in the following section. For much lower damping, say  $\tilde{\lambda} \lesssim 10^{-6}$ , which can be achieved in laboratory experiments, the steady state takes a long time to be reached. In those cases, it may be appropriate to modify our perturbative expansion by setting  $\tilde{\lambda} = \mathcal{O}(\Delta^n)$  with  $n > 1$ , or just solve (6) numerically for the entire time evolution, including the long transient state.

### 3.5 Numerical results

We now turn to comparing numerical solutions to (6) with the perturbative ones found in the previous sections. We numerically solved (6) with standard commercial software [34] over an interval  $0 \leq \tau \leq \tau_{\max}$  with  $\tau_{\max} \gg 1/\tilde{\lambda}$ , with appropriate initial conditions. The type of steady state reached by the system is insensitive to  $\theta(0)$  in most cases, but may be sensitive to  $d\theta/d\tau(0)$  depending on the values of  $\Delta$  and  $\tilde{\lambda}$ .

In figure 1 we show steady-state rotations for three different values of  $\Delta$  and  $\tilde{\lambda}$ . With  $\Delta = 0.1$  and  $2\tilde{\lambda}/\Delta = 0.2$ , as shown in figure 1 (a), the first-order approximation  $\theta_1(\tau)$  from (21) already agrees almost exactly with the numerical solution. For these parameter values we numerically find steady-state rotations for any value of  $\theta(0)$ , and for  $0.64 \leq d\theta/d\tau(0) \leq 2.13$ . Outside of that range of initial angular velocities the steady states we obtain numerically are the equilibria  $\theta(\tau) = n\pi$ .

In figure 1 (b) we set  $\Delta = 0.8$  and  $2\tilde{\lambda}/\Delta = 0.025$ . The first-order approximation is very close to the numerical solution, and the second-order one  $\theta_2(\tau)$  is indistinguishable from it. We numerically find steady-state rotations for any  $\theta(0) \neq 2n\pi$ , and for all values of  $10^{-6} \lesssim d\theta/d\tau(0) \lesssim 10^3$  we tried.

Numerical analysis of (6) shows that the steady-state rotations described in section 3.2 for  $\Delta \lesssim 1$  exist also for larger values of  $\Delta$ , although the perturbative expansion discussed there is not directly applicable when  $\Delta \gg 1$ . (In the latter case, an expansion in powers of  $1/\Delta$  would be appropriate.) Nevertheless, as discussed at the end of section 3.2, the form of the expansion suggests that it may converge even for  $\Delta \gtrsim 1$ . This is shown in figure 1 (c), where  $\Delta = 2.3$  and  $2\tilde{\lambda}/\Delta = 0.61$ . As seen in the figure, the agreement between the numerical and the perturbative solutions is very accurate at third order. Also, each successive perturbative order gives a significant improvement over the previous one, signalling good convergence of perturbation theory even at such large values of  $\Delta$  (as long as damping is also sufficiently large). In this case we also find steady-state rotations for any  $\theta(0) \neq 2n\pi$ , and for all values of  $d\theta/d\tau(0)$  over many orders of magnitude.

The steady-state rotations described in section 3.2 and in figures 1 (a), (b), (c), exist for large open sets in parameter space, even in the perturbative regime  $\Delta, \tilde{\lambda} \lesssim 1$ , and are reached by the system for relatively large open sets of initial conditions, as described above. The steady-state oscillations described in section 3.3, by contrast, are found numerically only for  $\Delta \ll \tilde{\lambda}$ . Under those conditions, the angular velocity quickly reaches its typical steady-state magnitude and, as a result, the mean value of  $\theta$  evolves very slowly towards its steady-state value and numerical solutions are computationally expensive. Also, unlike steady rotations, these oscillating steady-states are not robust in the sense that even small variations in the initial velocity may lead the system away from them and towards an equilibrium solution. An example of steady-state oscillations about  $\pi/2$  is shown in figure 1 (d). In that case the numerical result is well described by the first-order solution (23) and, in the figure, indistinguishable from the second-order one (24).

## 4 Elliptically excited parametric rotator

The simplest implementation of a parametric rotator is probably the well-known toy model described in [35] as a “rotator on a notched stick.” In that case the trajectory of the suspension is well approximated by a highly eccentric ellipse. The elliptical excitation of the parametric rotator is of interest by itself, and also because it continuously connect the cases of linear ( $\epsilon = 0$ ) and circular ( $\epsilon = \pm\pi/2$ ) excitations, that lead to rather different types of steady states. In this section we consider the extension of the results of section 3 to the case of elliptic motion of the suspension point.

The equation of motion (4), without gravity, takes the form,

$$\frac{d^2\theta}{d\tau^2} + \tilde{\lambda}\frac{d\theta}{d\tau} + \frac{\Delta}{2}(1 - \sin\epsilon)\sin(\theta + \tau) + \frac{\Delta}{2}(1 + \sin\epsilon)\sin(\theta - \tau) = 0, \quad (26)$$

where  $-\pi/2 \leq \epsilon \leq \pi/2$ . For  $\epsilon = 0$  the suspension point oscillates along a line segment, and we recover (6). For  $0 < \epsilon < \pi/2$  the suspension point moves counterclockwise along an elliptic orbit, which becomes circular at  $\epsilon = \pi/2$ . Similarly, negative values  $-\pi/2 \leq \epsilon < 0$  describe clockwise motion of the suspension point. In this paper we restrict ourselves mostly to eccentric elliptic excitations,  $|\epsilon| \lesssim 1/2$  that are close to the linear case considered in previous sections. Circular, or slightly-eccentric elliptic, motions of the suspension point ( $1 \lesssim |\epsilon| \leq \pi/2$ ) lead to qualitatively different solutions that will be discussed elsewhere [36].

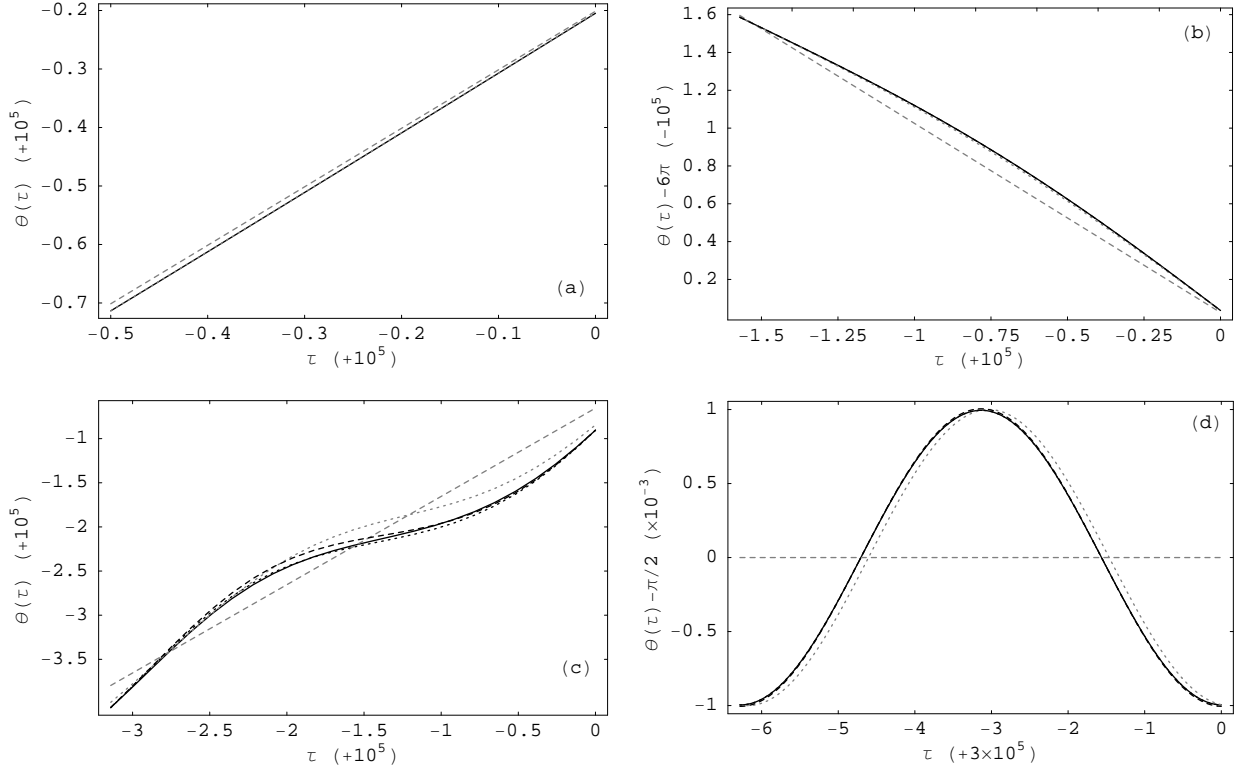


Figure 1: Numerical solution (black solid line) to equation (6), compared with perturbative solutions at zeroth (grey dashed line), first (grey dotted line), second (black dashed line) and third (black dotted line) orders as given in section 3. Steady-state rotations (see section 3.2: (a)  $\Delta = 0.1$ ,  $\tilde{\lambda} = 0.01$ ,  $\theta(0) = 0$ ,  $d\theta/d\tau(0) = 0.7$ ; (b)  $\Delta = 0.8$ ,  $\tilde{\lambda} = 0.01$ ,  $\theta(0) = 0$ ,  $d\theta/d\tau(0) = 0.001$ ; (c)  $\Delta = 2.3$ ,  $\tilde{\lambda} = 0.7$ ,  $\theta(0) = -0.1$ ,  $d\theta/d\tau(0) = 1$ . Steady-state oscillations (see section 3.3): (d)  $\Delta = 0.001$ ,  $\tilde{\lambda} = 0.1$ ,  $\theta(0) = \pi/2$ ,  $d\theta/d\tau(0) = 0$ .

Equation (26) is invariant under the transformation  $\theta \rightarrow -\theta$ ,  $\epsilon \rightarrow -\epsilon$ . Thus, if  $\theta(\tau, \epsilon)$  is a solution to (26) for some  $\epsilon$ , then  $-\theta(\tau, -\epsilon)$  is also a solution for the same  $\epsilon$ . There are no equilibrium solutions to (26) when  $\epsilon \neq 0$ . When  $\epsilon = 0$ , the linear case, the equilibria are  $\theta(\tau) = n\pi$ , with integer  $n$ .

#### 4.1 Steady-state rotations

We now look for counter-clockwise steady-state rotations of the form (12). Let  $\theta(\tau, \epsilon_0)$  be such a solution for  $\epsilon = \epsilon_0 > 0$ . Since both the rotator and suspension point move in the same sense, we will say that  $\theta(\tau, \epsilon_0)$  describes a ‘‘direct motion’’ of the rotator. By symmetry,  $-\theta(\tau, -\epsilon_0)$  is a solution of (26) with  $\epsilon = \epsilon_0$ , describing a clockwise motion of the rotator with a counter-clockwise moving suspension point, what we call a ‘‘contrarian motion’’ of the rotator. Similarly,  $\theta(\tau, -\epsilon_0)$  and  $-\theta(\tau, \epsilon_0)$  are solutions to (26) with  $\epsilon = -\epsilon_0 < 0$ , describing contrarian and direct motion, respectively.

After substituting (12) in (26), a straightforward application of the perturbative method of section 3 leads to the perturbative solution we seek. At lowest order we get

$$\theta_0(\tau) = \tau + \Theta_0, \quad \Theta_0 = -\arcsin\left(\frac{2}{1 + \sin \epsilon} \frac{\tilde{\lambda}}{\Delta}\right) + 2n\pi. \quad (27)$$

Therefore, in this case steady-state rotations occur only if

$$\tilde{\lambda} < \frac{\Delta}{2}(1 + \sin \epsilon), \quad (28)$$

which generalises condition (11) to elliptic excitations of the rotator. We see also that contrarian motions are allowed by (28), for small enough  $\tilde{\lambda}$ , except for  $\epsilon = -\pi/2$ . Thus, for circular parametric excitation there can be no contrarian motion.

At first order we get,

$$\theta_1(\tau) = \theta_0(\tau) + \Delta f_1(\tau), \quad f_1(\tau) = \frac{1}{8}(1 - \sin \epsilon) \sin(2\tau + \Theta_0). \quad (29)$$

In particular,  $\Theta_1 = 0$  as in the linear-excitation case of section 3. The second-order solution takes the form,

$$\begin{aligned} \theta_2(\tau) &= \theta_1(\tau) + \frac{\Delta^2}{2}(\Theta_2 + f_2(\tau)), & \Theta_2 &= \frac{5}{27}(1 - \sin \epsilon)^2 \tan(\Theta_0), \\ f_2(\tau) &= \frac{3}{26}(\cos \epsilon)^2 \sin(2\tau) - \frac{1}{26}(\cos \epsilon)^2 \sin(2\tau + 2\Theta_0) + \frac{1}{28}(1 - \sin \epsilon)^2 \sin(4\tau + 2\Theta_0). \end{aligned} \quad (30)$$

Finally, at third order we obtain,

$$\begin{aligned} \theta_3(\tau) &= \theta_2(\tau) + \frac{\Delta^3}{3!}(\Theta_3 + f_3(\tau)), & \Theta_3 &= \frac{15}{29}(1 - \sin \epsilon)(\cos \epsilon)^2 \sin(\Theta_0), \\ f_3(\tau) &= \frac{3}{8}\Theta_2(1 - \sin \epsilon) \cos(2\tau + \Theta_0) + \frac{27}{2^{10}}(\cos \epsilon)^2(1 + \sin \epsilon) \sin(2\tau - \Theta_0) \\ &+ \frac{3}{2^{12}}(29(\sin \epsilon)^3 + 9(\sin \epsilon)^2 - 9\sin \epsilon - 29) \sin(2\tau + \Theta_0) + \frac{3}{2^{10}}(\cos \epsilon)^2(1 + \sin \epsilon) \sin(2\tau + 3\Theta_0) \\ &+ \frac{45}{2^{14}}(\cos \epsilon)^2(1 - \sin \epsilon) \sin(4\tau + \Theta_0) - \frac{15}{2^{14}}(\cos \epsilon)^2(1 - \sin \epsilon) \sin(4\tau + 3\Theta_0) \\ &+ \frac{1}{2^{12}}(1 - \sin \epsilon)^3 \sin(6\tau + 3\Theta_0). \end{aligned} \quad (31)$$

Some remarks on these expressions are in order. First, at  $\epsilon = 0$  the perturbative solution described above reduces to the one found in section 3.2 for the case of linear excitation. Second, at  $\epsilon = \pi/2$  the perturbative corrections  $\Theta_{2,3}$  and  $f_{1,2,3}(\tau)$  vanish. In fact, all  $\Theta_n$ ,  $f_n(\tau)$ ,  $n \geq 1$ , must vanish in that case because for circular excitation  $\theta_0(\tau)$ , as given by (27), is an exact solution to (26). Third, only even angular frequencies enter the perturbative corrections.

## 4.2 Steady-state oscillations

We now look for solutions to (26) of the form (22). Assuming  $\Delta, \tilde{\lambda} \lesssim 1$ , and substituting (22) in (26), leads us to a perturbative analysis completely analogous to that of section 3.3, so we omit the details for brevity. From (22) we have the zeroth-order solution

$$\theta_0(\tau) = \Theta_0, \quad (32)$$

with  $\Theta_0$  undetermined at this order. The first-order equation yields,

$$f_{(g)1}(\tau) = -\frac{1}{2}(1 + \sin \epsilon) \sin(\tau - \Theta_0) + \frac{1}{2}(1 - \sin \epsilon) \sin(\tau + \Theta_0), \quad (33)$$

Consistency of the second-order equation requires  $\cos \epsilon \sin(2\Theta_0) = 0$ , therefore,

$$\Theta_0 = \frac{1}{2}k\pi, \quad \text{if } \cos \epsilon \neq 0, \quad (34)$$

for some integer  $k$ . In the case of circular excitation,  $\cos \epsilon = 0$ ,  $\Theta_0$  as well as all  $\Theta_n$  remain undetermined due to the invariance of (26) under a one-parameter continuous symmetry. The details of that particular case will be discussed elsewhere [36]. With  $\Theta_0$  given by (34), the equation for  $f_2$  leads to,

$$\begin{aligned} f_2(\tau) = & (\Theta_1 - \tilde{\lambda}/\Delta)(1 + \sin \epsilon) \cos(\tau - \Theta_0) + (\Theta_1 + \tilde{\lambda}/\Delta)(1 - \sin \epsilon) \cos(\tau + \Theta_0) \\ & - \frac{1}{16}(1 + \sin \epsilon)^2 \sin(2\tau - 2\Theta_0) + \frac{1}{16}(1 - \sin \epsilon)^2 \sin(2\tau + 2\Theta_0). \end{aligned} \quad (35)$$

The constant  $\Theta_1$ , undetermined at this order, is fixed by the consistency requirement for the third-order equation

$$\Theta_1 = \frac{\tilde{\lambda}}{\Delta} \frac{\sin \epsilon}{(\cos \epsilon)^2} \cos(2\Theta_0). \quad (36)$$

With this value for  $\Theta_1$  we obtain a bounded solution  $f_3(\tau)$  to the third-order equation. We omit the expression for  $f_3(\tau)$ , however, because it is too lengthy to transcribe here. Finally,

$$\Theta_2 = 0 \quad (37)$$

is required for consistency of the fourth-order equation.

For  $\epsilon = 0$  these solutions must satisfy (6). Thus, setting  $k = 2n$  in (34) leads to  $\Theta_0 = n\pi$ , and we recover the equilibrium solutions of the linear case. In particular, all corrections  $\Theta_i, f_i, i \geq 1$  must vanish, since  $\Theta_0$  is an exact solution to (6) in this case. It is easily seen that this indeed happens with the corrections (33) and (35)–(37). On the other hand, by setting  $k = 2n + 1$  in (34) we recover the oscillating solutions discussed in section 3.3.

## 4.3 Numerical results

The perturbative results for elliptic motion of the suspension point are compared to numerical solutions to (26) in figure 2. Figure 2 (a) shows a contrarian steady-state rotation, with  $\epsilon = -1/2$  and  $\Delta = 0.1$ . Because the oscillation amplitude is small we plotted  $\theta(\tau) - \tau$  instead of  $\theta(\tau)$ . The zeroth-order solution (27) is then shown in the figure as  $\theta_0(\tau) - \tau = \Theta_0 \simeq -0.876$ . As also seen there, the first-order result (29) is very close to the numerical solution, and the second-order result (30) agrees exactly with it.

For the contrarian motion with  $\theta(0) = 0$  shown in figure 2 (a) we find steady rotations for  $0.987 \leq d\theta/d\tau(0) \leq 1.090$ . For other values of  $d\theta/d\tau(0)$  the steady state is oscillatory, about  $n\pi$  for some integer  $n$ . Although not shown in the figure, we mention here that for  $\theta(0) = \pi/8$  and  $\pi/4$  we could not find steady-state rotations, any  $d\theta/d\tau(0)$  leading to steady oscillations about  $n\pi$  instead. If we set  $\Delta$  and  $\tilde{\lambda}$  to the same values as in figure 2 (a), but  $\epsilon = +1/2$ , then with  $\theta(0) = 0$  steady-state rotations are reached for  $0.559 \leq d\theta/d\tau(0) \leq 1.519$ , with  $\theta(0) = \pi/8$  for  $0.579 \leq d\theta/d\tau(0) \leq 1.483$ , and with  $\theta(0) = \pi/4$  for  $0.624 \leq d\theta/d\tau(0) \leq 1.419$ . These numerical results suggest that the interval of initial angular velocities leading to steady-state rotations decreases in length with increasing  $\theta(0)$ . Also, as intuitively expected, for fixed  $\theta(0)$  that length is larger for direct than for contrarian motion.

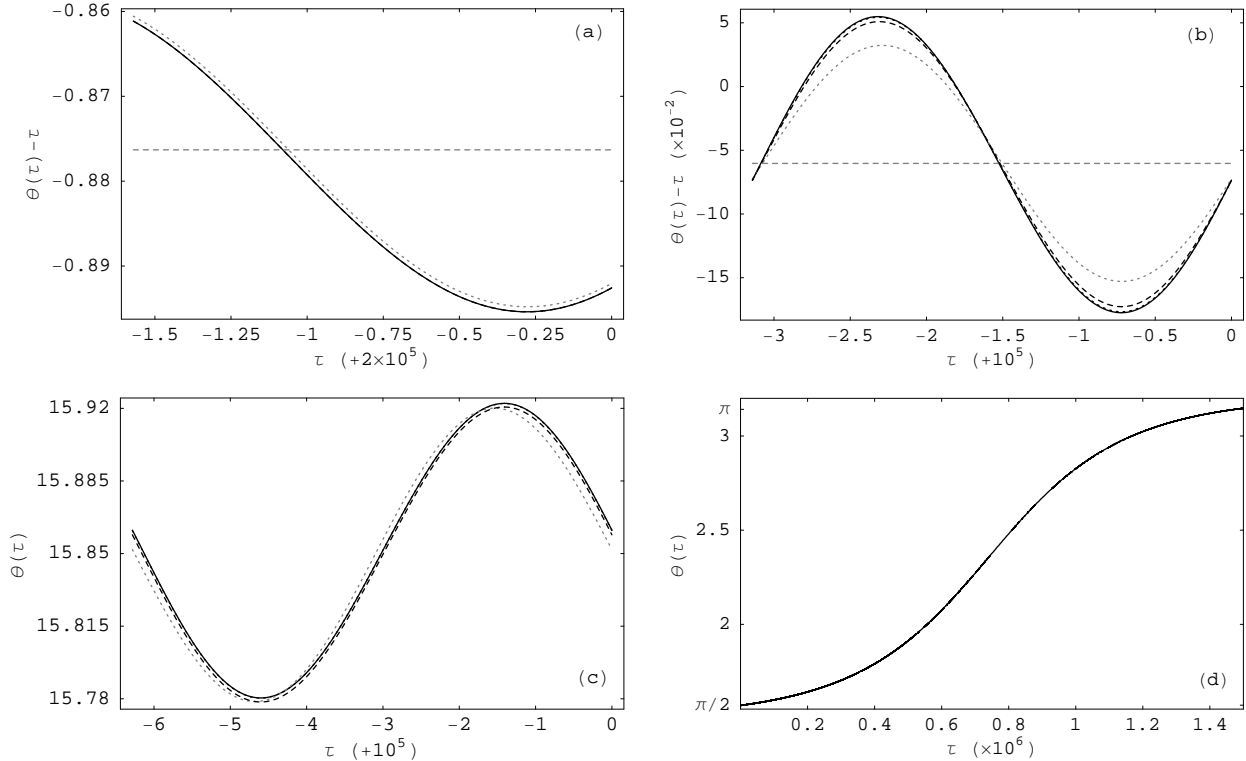


Figure 2: Numerical solution (black solid line) to equation (26), compared with perturbative solutions at zeroth (grey dashed line), first (grey dotted line), second (black dashed line) and third (black dotted line) orders as given in section 4. Steady-state rotations (see section 4.1): (a)  $\epsilon = -0.5$ ,  $\Delta = 0.1$ ,  $\tilde{\lambda} = 0.02$ ,  $\theta(0) = 0, d\theta/d\tau(0) = 1$ ; (b)  $\epsilon = \pi/8$ ,  $\Delta = 1.2$ ,  $\tilde{\lambda} = 0.05$ ,  $\theta(0) = 0$ ,  $d\theta/d\tau(0) = 1$ . Steady-state oscillations (see section 4.2): (c)  $\epsilon = \pi/4$ ,  $\Delta = 0.1$ ,  $\tilde{\lambda} = 0.1$ ,  $\theta(0) = 0$ ,  $d\theta/d\tau(0) = 1$ ; (d)  $\epsilon = \pi/6$ ,  $\Delta = 0.001$ ,  $\tilde{\lambda} = 0.1$ ,  $\theta(0) = \pi/2$ ,  $d\theta/d\tau(0) = -1.33 \times 10^{-4}$ .

In figure 2 (b) we show a direct steady-state rotation, with  $\epsilon = \pi/8$  and  $\Delta = 1.2$ . In this case the zeroth-order result (27) is given by  $\Theta_0 = -6 \times 10^{-2}$ . Like in the case of linear excitation, we see that perturbation theory converges for  $\Delta \gtrsim 1$ . As seen in the figure, the second-order result (30) accurately reproduces the numerical solution, and the third-order result (31) cannot be distinguished from the numerical one. For these values of the parameters we found steady-state rotations for any value of  $\theta(0)$  and for any  $0 \leq d\theta/d\tau(0) \leq 10^3$ .

We show a steady-state oscillating solution in figure 2 (c), with  $\epsilon = \pi/4$ ,  $\Delta = 0.1 = \tilde{\lambda}$ . In this case condition (28) is violated, so steady rotations are not possible. The value of  $\Theta_0 = 5\pi \simeq 15.708$  receives corrections  $\Delta\Theta_1, \Delta^3/6\Theta_3$ , so that the solution oscillates about  $\Theta \simeq 15.851$ . The accuracy of the perturbative results from section 4.2 is apparent in the figure, where no departure of the third-order result from the numerical solution is visible.

In the case of linear excitation ( $\epsilon = 0$ ), as discussed in section 3.5, steady-state solutions oscillating about  $(2n+1)\pi/2$  could be found (see figure 1 (d)), although finding them required some degree of fine-tuning of initial conditions. For  $\epsilon \neq 0$  those solutions seem to be unstable. An example is shown in figure 2 (d), with  $\epsilon = \pi/6$ , where the solution initially oscillates about  $\Theta = \pi/2$  but moves away from that value to end up oscillating about  $\Theta = \pi$ . For smaller values of  $\epsilon$  the growth of the mean value of  $\theta(\tau)$  from  $\pi/2$  is slower, but even for  $\epsilon$  as low as  $10^{-4}$  we could not find numerically a stable solution of this type.

## 5 Elliptically excited parametric pendulum

In the general case of elliptic motion of the suspension point, with the  $z$  axis chosen along the major axis of the ellipse and with the direction of gravity at an angle  $\pi + \alpha$  with that axis, equation (4) takes the form

$$\frac{d^2\theta}{d\tau^2} + \tilde{\lambda}\frac{d\theta}{d\tau} + \frac{\Delta}{2}(1 - \sin\epsilon)\sin(\theta + \tau) + \frac{\Delta}{2}(1 + \sin\epsilon)\sin(\theta - \tau) + \Gamma\sin(\theta + \alpha) = 0. \quad (38)$$

This equation is invariant under the transformation  $\theta \rightarrow -\theta$ ,  $\epsilon \rightarrow -\epsilon$ ,  $\alpha \rightarrow -\alpha$ . Thus, if  $\theta(\tau, \epsilon, \alpha)$  is a solution to (38) for some  $\epsilon$ ,  $\alpha$ , then  $-\theta(\tau, -\epsilon, -\alpha)$  is also a solution for the same  $\epsilon$ ,  $\alpha$ . There are no equilibrium solutions to (38) when either  $\epsilon \neq 0$  or  $\alpha \neq 0$ . For  $\epsilon = 0 = \alpha$  the equilibria are  $\theta(\tau) = n\pi$ , with integer  $n$ , as in the case  $\Gamma = 0$ .

When  $\Delta$ ,  $\tilde{\lambda}$ ,  $\Gamma \lesssim 1$  we can solve (38) perturbatively for the steady-state solution along the same lines as in the previous sections. The parameter  $\Gamma$  defined in (5) may be made arbitrarily small by tilting the plane of the rotator with respect to the vertical, so that  $g$  itself is small; or by making  $\gamma$  large,  $\gamma > \sqrt{g/L}$ ; or by making small the rotator asymmetry  $((L_1 - L_2)/L$  in the case of the thin homogeneous bar discussed in section 2). For arbitrary, but small, values of the parameters, we discuss below steady-state rotations and two different oscillation regimes. Furthermore, for  $\Gamma \simeq 1/4$ , there are two additional types of solutions that we discuss in section 6.

### 5.1 Steady-state rotations

The equation of motion (38) admits solutions of the form (12), which we will denote by  $\theta_{(g)}(\tau)$  to distinguish them from the solutions  $\theta(\tau)$  obtained in section 4 for  $\Gamma = 0$ . Like in that section, we need only consider positive angular frequency solutions  $\theta_{(g)}(\tau, \epsilon, \alpha)$ ,  $\epsilon > 0$ , describing direct counterclockwise rotations. Clockwise rotations are then given by  $-\theta_{(g)}(\tau, -\epsilon, -\alpha)$ . For the purpose of perturbation theory we consider  $\Delta$ ,  $\tilde{\lambda}$  and  $\Gamma$  to be small of the same order. In particular,  $\Gamma/\Delta$  and  $\tilde{\lambda}/\Delta$  both remain finite as  $\Delta \rightarrow 0$ . The perturbative computation is a simple extension of the analyses of sections 3.2 and 4.1, so we omit the details for brevity, limiting ourselves to quoting the results through second order. At zeroth order we have

$$\theta_{(g)0}(\tau) = \theta_0(\tau), \quad (39)$$

with  $\theta_0(\tau)$  given by (27), so  $\Theta_0$  is independent of  $\Gamma$  and relation (28) holds unchanged. In particular, for circular excitation there can be no contrarian motion, as in the case  $\Gamma = 0$ . At first order,

$$\theta_{(g)1}(\tau) = \theta_1(\tau) + \Gamma f_{(g)1}(\tau), \quad f_{(g)1}(\tau) = \sin(\tau + \Theta_0 + \alpha), \quad (40)$$

with  $\theta_1(\tau)$  given in (29). At second order we get,

$$\theta_{(g)2}(\tau) = \theta_{(g)1}(\tau) + \frac{1}{2}\Delta^2 f_2(\tau) + \frac{1}{2}\Delta^2 \Theta_2 + \frac{1}{2}\Gamma^2 f_{(g)2}(\tau) + \frac{1}{2}\Gamma^2 \Theta_{(g)2}, \quad (41a)$$

with  $f_2(\tau)$  and  $\Theta_2$  as defined in (30) and,

$$\begin{aligned} \Theta_{(g)2} &= \left( \frac{3}{2} \tan(\Theta_0) - \frac{1}{8} \frac{1 - \sin(\epsilon)}{1 + \sin(\epsilon)} \frac{\sin(\Theta_0 + 2\alpha)}{\cos(\Theta_0)} \right), \\ f_{(g)2}(\tau) &= -\frac{3}{8} \frac{\Delta}{\Gamma} (1 - \sin\epsilon) \sin(\tau - \alpha) + \frac{\Delta}{\Gamma} (1 + \sin\epsilon) \sin(\tau + \alpha) \\ &\quad + \frac{5}{72} \frac{\Delta}{\Gamma} (1 - \sin\epsilon) \sin(3\tau + 2\Theta_0 + \alpha) + \frac{1}{4} \sin(2\tau + 2\Theta_0 + 2\alpha). \end{aligned} \quad (41b)$$

Notice that in this equation we have eliminated  $\tilde{\lambda}$  in favour of  $\Theta_0$ .

A qualitative change with respect to the result of section 4 with  $\Gamma = 0$  is that the corrections  $f_{(g)n}$  coming from gravity contain odd frequencies, so  $\theta_{(g)}(\tau) - \tau$  has period  $2\pi$ . We notice also that the phase of  $\theta_{(g)}(\tau)$  acquires a dependence on  $\Gamma$  at second order. The perturbative solution to (38) described by (39) — (41) exists only if (28) is satisfied, due to the definition (27) of  $\Theta_0$ .

## 5.2 Steady-state oscillations ( $\Gamma \sim \Delta$ )

We look for steady-state solutions of the form (22). As in the previous section, we consider  $-\pi/2 \leq \epsilon \leq \pi/2$  thus including the case of circular excitation. For the purpose of the perturbative calculation we assume  $\Delta, \tilde{\lambda}, \Gamma \lesssim 1$  to be small of the same order. From (38) and (22) we find the zeroth-order solution

$$\theta_{(g)0}(\tau) = \Theta_{(g)0} = n\pi - \alpha, \quad (42)$$

with integer  $n$ . The value of  $\Theta_{(g)0}$  results from consistency of the first-order equation, which then yields the first-order solution

$$\theta_{(g)1}(\tau) = \Theta_{(g)0} + \Delta\Theta_{(g)1} + \Delta f_{(g)1}(\tau), \quad (43a)$$

with  $f_{(g)1}(\tau)$  given by (33) and, from the requirement that  $f_{(g)2}(\tau)$  be bounded,

$$\Theta_{(g)1} = -\frac{1}{4} \left( \frac{\Delta}{\Gamma} \right) (\cos \epsilon)^2 \frac{\sin(2\Theta_{(g)0})}{\cos(\Theta_{(g)0} + \alpha)}. \quad (43b)$$

The second-order equation leads to

$$\theta_{(g)2}(\tau) = \theta_{(g)1}(\tau) + \frac{\Delta^2}{2}\Theta_{(g)2} + \frac{\Delta^2}{2}f_{(g)2}(\tau), \quad (44a)$$

with

$$\begin{aligned} \Theta_{(g)2} &= \frac{1}{\cos(\Theta_{(g)0} + \alpha)} \left( \frac{\tilde{\lambda}}{\Gamma} \sin \epsilon - \frac{1}{8}(\cos \epsilon)^2 \sin(\Theta_0 - \alpha) - \frac{3}{8}(\cos \epsilon)^2 \sin(3\Theta_{(g)0} + \alpha) \right. \\ &\quad \left. - \frac{\Delta}{\Gamma}\Theta_{(g)1}(\cos \epsilon)^2 \cos(2\Theta_{(g)0}) \right), \\ f_{(g)2}(\tau) &= \left( \Theta_{(g)1} - \tilde{\lambda}/\Delta \right) (1 + \sin \epsilon) \cos(\tau - \Theta_{(g)0}) + \left( \Theta_{(g)1} + \tilde{\lambda}/\Delta \right) (1 - \sin \epsilon) \cos(\tau + \Theta_{(g)0}) \\ &\quad + \frac{\Gamma}{2\Delta} \left( (1 - \sin \epsilon) \sin(\tau - \alpha) - (1 + \sin \epsilon) \sin(\tau + \alpha) \right) \\ &\quad + \frac{\Gamma}{2\Delta} \left( (1 - \sin \epsilon) \sin(\tau + 2\Theta_{(g)0} + \alpha) - (1 + \sin \epsilon) \sin(\tau - 2\Theta_{(g)0} - \alpha) \right) \\ &\quad + \frac{1}{16} \left( (1 - \sin \epsilon)^2 \sin(2\tau + 2\Theta_{(g)0}) - (1 + \sin \epsilon)^2 \sin(2\tau - 2\Theta_{(g)0}) \right), \end{aligned} \quad (44b)$$

where  $\Theta_{(g)2}$  results from requiring consistency of the third-order equation.

In the case  $\epsilon = 0 = \alpha$ , corresponding to linear excitation in the same direction as gravity,  $\theta_{(g)0}(\tau)$  is an exact solution to (38), the equilibrium solution. In that case the corrections  $\Theta_{(g)1,2}, f_{(g)1,2}$  given in (43), (44) vanish, as must happen to all higher-order corrections  $\Theta_{(g)i}, f_{(g)i}$  with  $i \geq 2$ . For  $\epsilon \neq 0$  or  $\alpha \neq 0$  equations (42)–(44) describe steady-state oscillations with dimensionless fundamental angular frequency 1 (in physical units, angular frequency  $\gamma$ ) about a central value  $\Theta_{(g)} = \Theta_{(g)0} + \Delta\Theta_{(g)1} + \Delta^2/2\Theta_{(g)2} + \mathcal{O}(\Delta^3)$ . For  $n$  even in (42), the zeroth-order value  $\Theta_0$  corresponds to the direction of gravity on the plane of the rotator. By numerically solving (38) we find that the solutions with  $n$  odd are unstable in this regime  $\Gamma \sim \Delta$ , as expected.

This perturbative solution is generally valid for  $\Delta, \tilde{\lambda}, \Gamma$  small, independently of whether condition (28) is satisfied. If (28) holds, the steady state rotations of section 5.1 also exist and the system may reach one or the other steady state depending on its initial conditions.

## 5.3 Steady-state oscillations ( $\Gamma \ll \Delta$ )

The perturbative solution (42)–(44) given in the previous section was obtained under the assumption  $\Gamma = \mathcal{O}(\Delta)$ . In particular, its limit as  $\Gamma \rightarrow 0$  is not well defined. For  $\Gamma \ll \Delta$  perturbation theory must be accordingly modified, which we do in this section. We focus our discussion on the specific case  $\Delta < 1, \tilde{\lambda} = \mathcal{O}(\Delta), \Gamma = \mathcal{O}(\Delta^3)$ . (Many other regimes are of course possible, which lead to results analogous to those obtained here.) With those assumptions for the parameters and (22) for  $\theta_{(g)}(\tau)$ , we solve (38) perturbatively. At zeroth order the solution is a constant,  $\theta_{(g)0}(\tau) = \Theta_{(g)0}$ , to be determined. At order  $\Delta$ ,

$$\theta_{(g)1}(\tau) = \Theta_{(g)0} + \Delta\Theta_{(g)1} + \Delta f_{(g)1}(\tau), \quad (45)$$

with  $f_{(g)1}(\tau)$  given by (33), and both  $\Theta_{(g)0,1}$  still undetermined. Consistency of the  $\mathcal{O}(\Delta^2)$  equation requires  $\cos(\epsilon)^2 \sin(2\Theta_0) = 0$ , so that for  $\epsilon \neq \pm\pi/2$

$$\Theta_{(g)0} = \frac{n}{2}\pi, \quad (46)$$

for some integer  $n$ . With this, the second-order solution is

$$\begin{aligned} \theta_{(g)2}(\tau) &= \theta_{(g)1}(\tau) + \frac{\Delta^2}{2}(\Theta_{(g)2} + f_{(g)2}(\tau)), \\ f_{(g)2}(\tau) &= -\left(\frac{\tilde{\lambda}}{\Delta} - \Theta_{(g)1}\right)(1 + \sin \epsilon) \cos(\tau - \Theta_{(g)0}) + \left(\frac{\tilde{\lambda}}{\Delta} + \Theta_{(g)1}\right)(1 - \sin \epsilon) \cos(\tau + \Theta_{(g)0}) \\ &\quad - \frac{1}{16}(1 + \sin \epsilon)^2 \sin(2\tau - 2\Theta_{(g)0}) + \frac{1}{16}(1 - \sin \epsilon)^2 \sin(2\tau + 2\Theta_{(g)0}). \end{aligned} \quad (47)$$

The third-order equation requires

$$\Theta_{(g)1} = \frac{1}{(\cos \epsilon)^2} \frac{1}{\cos(2\Theta_{(g)0})} \left( \frac{\tilde{\lambda}}{\Delta} \sin \epsilon - 2 \frac{\Gamma}{\Delta^3} \sin(\Theta_{(g)0} + \alpha) \right), \quad (48)$$

for  $f_{(g)3}$  to be bounded. The explicit expression for  $f_{(g)3}$  is rather lengthy, so we omit it for brevity. Finally, the  $\mathcal{O}(\Delta^4)$  equation leads to the consistency condition

$$\Theta_{(g)2} = -4 \frac{\Gamma}{\Delta^3} \frac{1}{(\cos \epsilon)^2} \frac{\cos(\Theta_{(g)0} + \alpha)}{\cos(2\Theta_{(g)0})} \Theta_{(g)1}. \quad (49)$$

Equations (45)–(49) yield a steady-state solution to (38) through second order in  $\Delta < 1$ . Clearly, this perturbative solution breaks down as  $|\epsilon|$  approaches the upper bound  $\epsilon_{\max}$  such that  $\Theta_{(g)1}$  becomes  $\sim 1$ . Numerical study of these oscillating solutions suggests that for  $\epsilon_{\max} \lesssim |\epsilon| \leq \pi/2$  they disappear from the spectrum of steady states. Therefore, as intuitively expected, the oscillations described in this section require an eccentric enough parametric excitation.

In the case of linear excitation perpendicular to gravity ( $\epsilon = 0$ ,  $\alpha = \pm\pi/2$ ) the central value  $\Theta_{(g)}$  about which the pendulum oscillates was obtained in [1, 20, 31] for  $\tilde{\lambda} = 0$ . Our result  $\Theta_{(g)} = \Theta_{(g)0} + \Delta\Theta_{(g)1} + \Delta^2/2\Theta_{(g)2}$  given by (46), (48) and (49) agrees with those references at order  $\Delta$  if we set  $\tilde{\lambda} = 0$  in (48), but further generalises it to the case  $\tilde{\lambda} > 0$ , to second order in  $\Delta$ , to any angle  $\alpha$ , and to any large enough eccentricity (i.e., small enough  $\epsilon$ ). The full solution (45)–(49), which gives the steady-state oscillations about the central value  $\Theta_{(g)}$  through order  $\Delta^2$ , provides a similar generalisation to the oscillations described in [18] for an inverted pendulum. From (46) we see that our results are applicable in the cases  $\Theta_{(g)0} = 2k\pi$  with integer  $k$  (normal pendulum) and  $\Theta_{(g)0} = (2k+1)\pi$  (inverted pendulum). As discussed in the next section, by numerically solving (38) the solutions with  $\Theta_{(g)0} = (2k+1)\pi/2$  are found to be unstable.

## 5.4 Numerical results

The steady-state rotations obtained perturbatively in section 5.1 are compared with numerical solutions to (38) in figures 3 (a) and (b). In figure 3 (a) we show  $\theta(\tau) - \tau$  for linear motion of the suspension point ( $\epsilon = 0$ ), at several angles  $\alpha$  with the direction of gravity. The zeroth-order result (39) is  $\Theta_0 \simeq -0.025$ , independently of  $\Gamma$  and  $\alpha$ . The first-order result (40) already accurately describes the numerical solution, with which the second-order result (41) overlaps completely. In figure 3 (b) we show  $\theta(\tau) - \tau$  for elliptic excitation with  $\epsilon = \pi/8$  perpendicular to gravity, both for direct and contrarian motion. The zeroth-order result (39) is  $\Theta_0 \simeq -0.018$  for direct and  $-0.040$  for contrarian motion. The first and second-order results are seen to be in tight agreement with the numerical solution.

In figures 3 (c) and (d) we show steady-state oscillations as described in section 5.2. The parameters used in figure 3 (c) do not violate the condition (28), but the initial angular velocity  $d\theta/d\tau(0) = 10^{-5}$  is too small for steady-state rotations (at  $\epsilon = \pi/8$ ). Numerically, for these parameters we find steady rotations for  $0.78 \leq d\theta/d\tau(0) \leq 1.44$  for  $\alpha = 3\pi/8$ ,  $0.75 \leq d\theta/d\tau(0) \leq 1.42$  for  $\alpha = 7/5$ , and  $0.65 \leq d\theta/d\tau(0) \leq 1.55$  for  $\alpha = \pi/2$ . The rotator oscillates about a central position  $\Theta_{(g)}$  whose zeroth-order value  $\Theta_0 = -\alpha$  is the direction of gravity, but receives small second-order corrections  $\Delta^2/2\Theta_{(g)2} = 10^{-3}$ ,  $6 \times 10^{-4}$  and  $10^{-5}$  for

$\alpha = 3\pi/8, 7/5$  and  $\pi/2$ , respectively. If instead of  $\epsilon = \pi/8$  we had chosen any other value  $-\pi/3 \leq \epsilon \leq \pi/4$ , the curves would vary by only a small amount. For  $|\epsilon| \gtrsim \pi/4$ , however, steady rotations are obtained even for the small initial angular velocity used here. Notice that for  $\epsilon = \pm\pi/2$  these oscillating solutions do not exist, so we expect that as  $\epsilon$  approaches those values the oscillating steady states should disappear from the spectrum of solutions. In figure 3 (d) we set the parameters to the same values as in figure 3 (c) except for a larger  $\tilde{\lambda}$ , so that condition (28) is violated, and a larger initial angular velocity. Except for the buildup of additional turns during the transient, as indicated in the figure, the plots look almost the same as those of figure 3 (c). This is due to the fact that  $\tilde{\lambda}$  enters the solutions of section 5.2 only at order  $\Delta^2$ .

The oscillating solutions for  $\Gamma \ll \Delta$  obtained in section 5.3 are illustrated in figure 4. We focus there on solutions with  $\Theta_{(g)0} = (2n + 1)\pi$ , describing the well-known phenomenon of the ‘‘inverted pendulum’’ (see the references cited in section 1 above). In the case of linear parametric excitation parallel to gravity ( $\epsilon = 0 = \alpha$ ), the exact solutions to (38)  $\theta(\tau) = n\pi$  with  $n$  odd become stable for  $\Gamma \ll \Delta$ . In figure 4 (a) we show one such solution, including the transient and the relaxation to the steady state  $\theta(\tau) = \pi$ . When  $\epsilon = 0 \neq \alpha$  there are no equilibria. In figure 4 (b) we show the oscillating steady state in that case, for various values of  $\alpha$ . For  $\epsilon = 0$  and  $\Theta_{(g)0} = \pi$  the first-order result (45) becomes constant, as shown in the figure, whereas the second-order result (47) accurately reproduces the numerical solution. The pendulum oscillates about  $\Theta_{(g)} = \Theta_{(g)0} + \Delta\Theta_{(g)1} + \Delta^2/2\Theta_{(g)2} + \dots \simeq \pi + 1.2 \times 10^{-2}, \pi + 2.3 \times 10^{-2}, \pi + 2.9 \times 10^{-2}, \pi + 3.1 \times 10^{-2}$ , for  $\alpha = \pi/8, \pi/4, 3\pi/8, \pi/2$ , respectively. We recall here that  $\Theta$  is measured with respect to the trajectory of the suspension point, not that of gravity. For example, when  $\alpha = \pi/2$ , figure 4 (b) shows that the pendulum is oscillating about an almost horizontal position. Similar results are obtained in the case of elliptic excitation, as shown in figures 4 (c) and (d) with  $\epsilon = \pi/8$  and  $\epsilon = \pi/4$ . In those figures we omitted the curves corresponding to  $\alpha = \pi/2$  for clarity, because they lie very close to those for  $\alpha = 3\pi/8$ . As can be seen in the figure, the oscillation amplitude depends on both  $\alpha$  and  $\epsilon$ . For  $\epsilon \gtrsim \pi/4$  higher orders beyond the second are needed to reproduce the numerical solutions and, as  $\epsilon$  approaches  $\pm\pi/2$ , perturbation theory becomes inapplicable. For  $\epsilon = \pm\pi/2$  the oscillating steady states described in sections 5.3 do not exist.

Finally, we notice that (46) allows solutions oscillating about  $\Theta_{(g)0} = (2n + 1)\pi/2$ . Numerical study shows that, for the values of  $\Gamma, \Delta, \tilde{\lambda}$  considered in figure 4, those solutions are unstable even for  $\epsilon = 0$ , and therefore they cannot describe steady states. We have also numerically solved (38) for many sets of parameter values in the regime  $\Gamma \ll \Delta \ll \tilde{\lambda}$ , with  $\epsilon = 0$  and several angles  $\alpha$ , and in all cases found the solutions to be unstable. That instability is of the same type as in the case  $\Gamma = 0$ , as shown in figure 2 (d): the central value  $\Theta_{(g)}$  about which  $\theta_{(g)}(\tau)$  oscillates is not constant, but its  $\tau$  dependence is slow compared to the period of oscillation. Thus, the oscillations with  $\Theta_{(g)0} = (2n + 1)\pi/2$  are well described by the perturbative solutions of section 5.3, but only up to an additive constant and for time intervals short compared with the time scales of variation of the central value  $\Theta_{(g)}$ .

## 6 Parametric resonance

Besides the steady-state solutions obtained in section 5, when the value of  $\Gamma$  is in the vicinity of  $(\ell/2)^2$ ,  $\ell$  integer, (38) possesses resonant solutions. In this section we describe in detail the first parametric resonance mode, with  $\Gamma \simeq 1/4$ . We assume  $\Delta \lesssim 1$ ,  $\tilde{\lambda} = \mathcal{O}(\Delta)$  and  $\Gamma = 1/4 + \delta$  with  $\delta = \mathcal{O}(\Delta)$ , and expand in powers of  $\Delta^{1/2}$  to find a solution of the form

$$\theta(\tau) = \Theta_0 + \sum_{k \geq 1} \Delta^{k/2} f_k(\tau) . \quad (50)$$

In this case it turns out to be more convenient not to separate explicitly from  $f_k(\tau)$  an additive constant term, as done in the expansions (12), (22). Substituting (50) into (38), at zeroth order we find  $\sin(\Theta_0 + \alpha) = 0$ . The zeroth-order solution is then,

$$\theta_0(\tau) = \Theta_0 = -\alpha + n\pi , \quad (51)$$

with integer  $n$ . At order  $\Delta^{1/2}$  the equation of motion (38) yields

$$\frac{d^2 f_1}{d\tau^2} + \frac{1}{4} \cos(n\pi) f_1(\tau) = 0 . \quad (52)$$

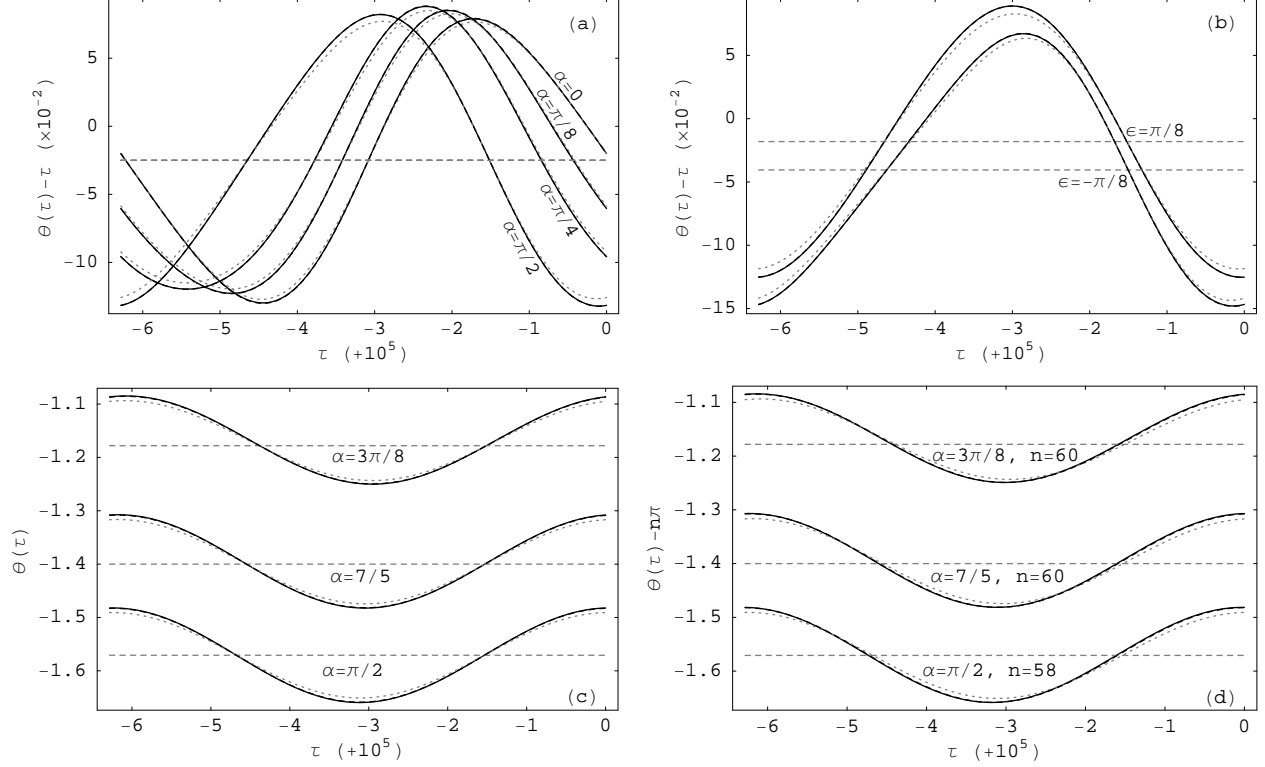


Figure 3: Numerical solution (black solid line) to equation (38), compared with perturbative solutions at zeroth (grey dashed line), first (grey dotted line) and second (black dashed line) orders as given in section 5. Steady-state rotations (see section 5.1): (a)  $\epsilon = 0$ ,  $\Gamma = 0.1$ ,  $\Delta = 0.08$ ,  $\tilde{\lambda} = 0.001$ ,  $\theta(0) = 0.1$ ,  $d\theta/d\tau(0) = 1.25$ ; (b)  $\epsilon = \pm\pi/8$ ,  $\alpha = \pi/2$ ,  $\Gamma = 0.1$ ,  $\Delta = 0.08$ ,  $\tilde{\lambda} = 0.001$ ,  $\theta(0) = 0.1$ ,  $d\theta/d\tau(0) = 1.25$ . Steady-state oscillations (see section 5.2): (c)  $\epsilon = \pi/8$ ,  $\Gamma = 0.1$ ,  $\Delta = 0.08$ ,  $\tilde{\lambda} = 0.001$ ,  $\theta(0) = 0.1$ ,  $d\theta/d\tau(0) = 10^{-5}$ ; (d)  $\epsilon = \pi/8$ ,  $\Gamma = 0.1$ ,  $\Delta = 0.08$ ,  $\tilde{\lambda} = 0.06$ ,  $\theta(0) = 0.1$ ,  $d\theta/d\tau(0) = 10$ .

Requiring  $f_1$  to be bounded leads to the condition that  $n$  in (51) must be even, so the pendulum oscillates at resonance about its position of lowest potential energy. The first-order solution is then,

$$\theta_1(\tau) = \Theta_0 + \Delta^{1/2} f_1(\tau), \quad f_1(\tau) = \rho_1 \cos(\tau/2 - \varphi_1), \quad (53)$$

with the constants  $\rho_1$ ,  $\varphi_1$  undetermined at this order. Similarly, the equation of motion at order  $\Delta$  is

$$\frac{d^2 f_2}{d\tau^2} + \frac{1}{4} f_2(\tau) = -\frac{1}{2}(1 - \sin \epsilon) \sin(\tau - \alpha) + \frac{1}{2}(1 + \sin \epsilon) \sin(\tau + \alpha), \quad (54)$$

leading to the second-order solution

$$\begin{aligned} \theta_2(\tau) &= \theta_1(\tau) + \Delta f_2(\tau), \\ f_2(\tau) &= \rho_2 \cos(\tau/2 - \varphi_2) + \frac{2}{3}(1 - \sin \epsilon) \sin(\tau - \alpha) - \frac{2}{3}(1 + \sin \epsilon) \sin(\tau + \alpha), \end{aligned} \quad (55)$$

with the constants  $\rho_2$ ,  $\varphi_2$  undetermined at this order. At  $\mathcal{O}(\Delta^{3/2})$  we obtain the equation for  $f_3(\tau)$

$$\begin{aligned} \frac{d^2 f_3}{d\tau^2} + \frac{1}{4} f_3(\tau) &= -\frac{\tilde{\lambda}}{\Delta} \frac{df_1}{d\tau} - \frac{\delta}{\Delta} f_1(\tau) + \frac{1}{24} f_1(\tau)^3 - \frac{1}{2}(1 - \sin \epsilon) \cos(\tau - \alpha) f_1(\tau) \\ &\quad - \frac{1}{2}(1 + \sin \epsilon) \cos(\tau + \alpha) f_1(\tau). \end{aligned} \quad (56)$$

The right-hand side of this equation, with  $f_1(\tau)$  given by (53), contains terms proportional to  $\cos(\tau/2)$  and  $\sin(\tau/2)$  leading to an unbounded solution  $f_3(\tau)$ . Requiring those terms to vanish determines the constants

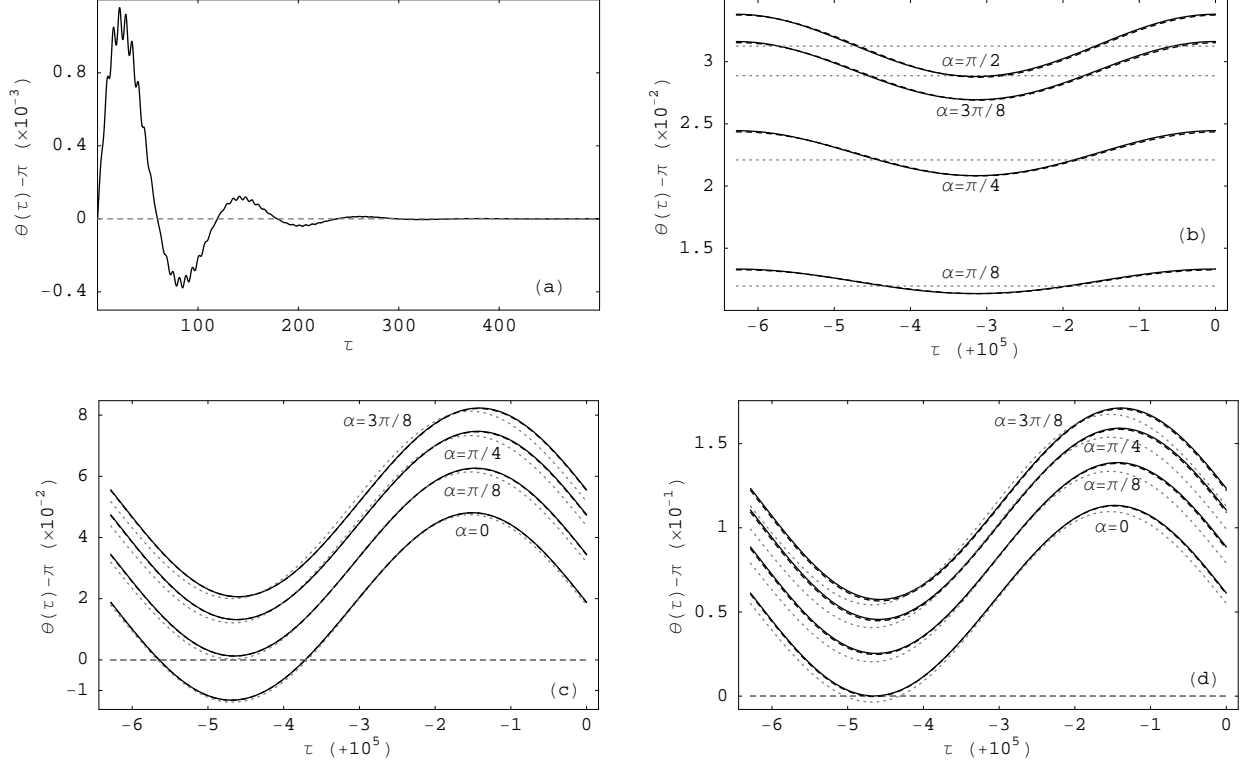


Figure 4: Inverted-pendulum solutions to equation (38). Numerical solution (black solid line), compared with perturbative solutions at zeroth (grey dashed line), first (grey dotted line) and second (black dashed line) orders as given in section 5.3. The parameters are set to  $\Gamma = 10^{-4}$ ,  $\Delta = 0.08$ ,  $\tilde{\lambda} = 0.0375$ ,  $\theta(0) = \pi$ ,  $d\theta/d\tau(0) = 10^{-4}$ , and (a)  $\epsilon = 0$ ,  $\alpha = 0$ ; (b)  $\epsilon = 0$ ; (c)  $\epsilon = \pi/8$ ; (d)  $\epsilon = \pi/4$ .

$\rho_1$ ,  $\varphi_1$  in (53) to be

$$\rho_1 = 4\sqrt{2\delta/\Delta + \sqrt{(\cos \alpha)^2 + (\sin \epsilon)^2(\sin \alpha)^2 - (\tilde{\lambda}/\Delta)^2}},$$

$$\varphi_1 = \arctan\left(\frac{-\cos \alpha + \sqrt{(\cos \alpha)^2 + (\sin \epsilon)^2(\sin \alpha)^2 - (\tilde{\lambda}/\Delta)^2}}{\tilde{\lambda}/\Delta - \sin \epsilon \sin \alpha}\right) + n_{\varphi_1}\pi, \quad (57)$$

where  $n_{\varphi_1}$  is an integer parameter on which the solution depends, similarly to the parameter  $n$  in (51). We remark, however, that from (53) it is apparent that the solutions depend only on whether  $n_{\varphi_1}$  is even or odd. With (57), equation (56) leads to a third-order solution of the form,

$$\theta_3(\tau) = \theta_2(\tau) + \Delta^{3/2}f_3(\tau),$$

$$f_3(\tau) = A_3 \sin(\tau/2) + B_3 \cos(\tau/2) - \frac{1}{192}\rho^3 \cos(3\tau/2 - 3\varphi_1) + \frac{1}{8}\rho(1 - \sin \epsilon) \cos(3\tau/2 - \alpha - \varphi_1) \quad (58)$$

$$+ \frac{1}{8}\rho(1 + \sin \epsilon) \cos(3\tau/2 + \alpha - \varphi_1).$$

The coefficients  $A_3$ ,  $B_3$  in  $f_3(\tau)$  are determined by the requirement that the perturbative equation of order  $\Delta^{5/2}$  must have a bounded solution. The resulting expressions are too lengthy to transcribe here, so we omit them (see, however, Appendix A). Finally, consistency of the equation at order  $\Delta^2$ , which determines  $f_4(\tau)$ , requires

$$\rho_2 = 0, \quad (59)$$

which fixes the second-order solution  $\theta_2(\tau)$  in (55). Summarising, the steady-state solution at order  $\Delta^0$  is given by (51); at order  $\Delta^{1/2}$  by (53) with (57); at order  $\Delta^1$  by (55) with (59); and at order  $\Delta^{3/2}$  by (58).

We remark that  $f_1(\tau)$  oscillates with angular frequency  $1/2$ , and  $f_2(\tau)$  with angular frequency  $1$ .  $f_{1,2}(\tau)$  determine the equations for the higher-order corrections  $f_k(\tau)$ ,  $k > 2$ . The structure of those perturbative equations is such that  $f_k(\tau)$  contains only terms with half-integer (respectively integer) angular frequency if  $k$  is odd (respectively even). As a consequence, the following relations, which are easily checked for the low-order solutions given above, actually persist to all orders of perturbation theory

$$\theta(\tau, \epsilon, \alpha, n_{\varphi_1} + 1) = -\theta(\tau, -\epsilon, -\alpha, n_{\varphi_1}) + 2n\pi = \theta(\tau + 2\pi, \epsilon, \alpha, n_{\varphi_1}) . \quad (60)$$

From the second equality we immediately see that in the case of linear motion of the suspension point parallel to gravity,  $\epsilon = 0 = \alpha$ , all terms with integer angular frequencies must vanish. In that case only the terms with odd  $k$  contribute to (50). In general, for arbitrary values of  $\epsilon$  and  $\alpha$ , equations (51)–(59) describe two different solutions according to whether  $n_{\varphi_1}$  is even or odd. Those two solutions are related, modulo  $2\pi$ , by the symmetries of (38) as shown by (60). Notice that, whereas the invariance of (38) under  $\theta(\tau) \rightarrow \theta(\tau + 2\pi)$  did not play any role in section 5 because there only integer angular frequencies appear, that symmetry acts non-trivially on the resonant solutions described in this section.

We see from (57) that there are two necessary conditions for these perturbative solutions to exist. The first one places an upper bound on damping for a given excitation amplitude,

$$\tilde{\lambda} \leq \Delta \sqrt{(\cos \alpha)^2 + (\sin \epsilon)^2 (\sin \alpha)^2} . \quad (61)$$

Thus, for linear excitation ( $\epsilon = 0$ ) there is no parametric resonance if  $\alpha = \pm\pi/2$ . For circular excitation the right-hand side of (61) becomes independent of  $\alpha$ , as expected. The second condition,

$$\delta > -\frac{1}{2}\Delta \sqrt{(\cos \alpha)^2 + (\sin \epsilon)^2 (\sin \alpha)^2 - (\tilde{\lambda}/\Delta)^2} , \quad (62)$$

puts a (negative) lower bound on  $\delta = \Gamma - 1/4$ . Notice that there is, apparently, no restriction on how large  $\delta$  can be as long as it is positive. This is, in fact, an artifact of perturbation theory: a non-perturbative stability analysis leads to well defined limits on the magnitude of  $\delta$  for resonance to be possible [21]. Yet, perturbation theory does restrict how negative  $\delta$  can be through (62). Numerical study confirms this asymmetric situation: given  $0 < \delta_0 \lesssim \Delta$  such that  $-\delta_0$  violates (62), resonant solutions can be found numerically for  $\delta = \delta_0$ , but not for  $\delta = -\delta_0$ .

## 6.1 Steady-state rotations with angular velocity $1/2$

When  $\Gamma = 1/4 + \delta$ , with  $\delta = \mathcal{O}(\Delta)$ ,  $\tilde{\lambda} \lesssim \Delta$  and  $\Delta \ll 1$ , equation (38) can be seen as a small perturbation about the unperturbed equation

$$\frac{d^2\theta}{d\tau^2} + \omega^2 \sin(\theta(\tau)) = 0 , \quad \omega = 1/2 . \quad (63)$$

In that case there must be solutions to (38) close to those of (63), with corrections of  $\mathcal{O}(\Delta)$ . For  $\omega^2 = 1/4$ , (63) possesses solutions of the form  $\theta(\tau) = \tau/2 + \Theta_0 + \sin(\tau/2 + \Theta_0) + \dots$ , for some constant  $\Theta_0$ , that can be computed perturbatively as an expansion in powers of  $\omega^2$ . How the remaining terms in (38) are added to (63) as perturbations depends on their relative size as compared to  $\omega^2 = 1/4$ . For  $\Delta \sim 10^{-2}$ – $10^{-1}$ ,  $\tilde{\lambda} \sim 10^{-3}$ – $10^{-2}$ ,  $\delta \sim \Delta$ , an appropriate expansion is obtained by setting  $\Delta = \mathcal{O}(\omega^4)$ ,  $\delta = \mathcal{O}(\omega^4)$  and  $\lambda = \mathcal{O}(\omega^6)$ . Thus, we expand (38) perturbatively, in a completely analogous way as in the previous sections, with

$$\theta(\tau) = \frac{1}{2}\tau + \Theta_0 + \sum_{n=1}^{\infty} (\omega^2)^n (\Theta_n + f_n(\tau)) . \quad (64)$$

At zeroth order we obtain,

$$\theta_0(\tau) = \frac{1}{2}\tau + \Theta_0 , \quad \Theta_0 = -\frac{1}{2} \arcsin \left( \frac{\tilde{\lambda}}{\Delta(1 + \sin \epsilon)} \right) - \frac{1}{2}\alpha + n\pi , \quad (65)$$

with  $n$  integer. We see that these steady states exist only if

$$\tilde{\lambda} \leq \Delta(1 + \sin \epsilon) . \quad (66)$$

At first order we get,

$$\theta_1(\tau) = \theta_0(\tau) + \frac{1}{4}(\Theta_1 + f_1(\tau)) , \quad \frac{1}{4}\Theta_1 = -2\delta \tan(2\Theta_0 + \alpha) , \quad \frac{1}{4}f_1(\tau) = \sin(\tau/2 + \Theta_0 + \alpha) . \quad (67)$$

We remark that this first-order solution already depends on all of the parameters in (38), and therefore on all of the physical quantities entering it: elliptic parametric excitation and gravity, their relative angle, and damping. Notice also that at this order (67) is a solution to (63), the additional terms in (38) entering (67) only through  $\Theta_{0,1}$ . At second order the perturbative solution is

$$\begin{aligned} \theta_2(\tau) &= \theta_1(\tau) + \frac{1}{16}(\Theta_2 + f_2(\tau)) , \\ \frac{1}{16}\Theta_2 &= -\frac{1}{\cos(2\Theta_0 + \alpha)} \frac{1}{1 + \sin \epsilon} \frac{\tilde{\lambda}}{4\Delta} - \delta\Theta_1 + \frac{1}{4}\tan(2\Theta_0 + \alpha) + \frac{1}{16}\Theta_1^2 \tan(2\Theta_0 + \alpha) , \\ \frac{1}{16}f_2(\tau) &= \frac{1}{8}\sin(\tau + 2\Theta_0 + 2\alpha) - 2\Delta(1 + \sin \epsilon) \sin(\tau/2 - \Theta_0) + \frac{2}{9}\Delta(1 - \sin \epsilon) \sin(3/2\tau + \Theta_0) \\ &\quad + 4\delta \sin(\tau/2 + \Theta_0 + \alpha) + \frac{1}{4}\Theta_1 \cos(\tau/2 + \Theta_0 + \alpha) . \end{aligned} \quad (68)$$

Because the expansion parameter  $\omega^2 = 1/4$  is not very small, the third-order correction is necessary in order to obtain a perturbative solution as accurate as those given in previous sections. We take into account the third-order terms in numerical computations in the following section, but we omit them here for brevity.

## 6.2 Numerical results

The previous results on parametric resonance are compared to numerical solutions to (38) in figure 5. The case of linear excitation parallel to gravity,  $\epsilon = 0 = \alpha$ , is shown in figure 5 (a), where we plot the order  $\Delta^{1/2}$  result (53), with (57), and the order  $\Delta^{3/2}$  result given in (58) and Appendix A. The parameters in that figure were chosen so  $\delta$  is very close to the bound (62) which in this case reduces to  $\delta = -0.047 > -0.05$ . This is the region where perturbation theory begins to break down, thus appropriate to test the  $\mathcal{O}(\Delta^{3/2})$  correction. As seen in the figure, the numerical solution is accurately reproduced by our perturbative result. For slightly higher values,  $\delta \geq -0.04$ , the  $\mathcal{O}(\Delta^{1/2})$  result would be enough to achieve the same accuracy.

In figure 5 (b) we illustrate the case of linear excitation not parallel to gravity,  $\epsilon = 0 \neq \alpha$ , for which the order  $\Delta^1$  correction (55), with (59), is non-vanishing. The agreement of the perturbative results with the numerical one is very accurate. The decreasing amplitude of oscillation with increasing  $\alpha$  is apparent from the figure. As discussed above, (61) implies that there is no resonance when gravity is perpendicular to the linear trajectory of the suspension point. This is confirmed in the figure, where the numerical solution with  $\alpha = \pi/2$  is seen to be an oscillating solution of the type described in section 5.2, with twice the frequency of the resonant solutions and a much smaller amplitude.

The case  $\epsilon \neq 0$  is shown in figure 5 (c), where we set  $\epsilon = \pi/2$  corresponding to counterclockwise circular motion of the suspension point. Unlike figure 5 (b), the oscillation amplitude does not show a discernible dependence with  $\alpha$ , and for  $\alpha = \pi/2$  a resonant solution is obtained. Aside from those quantitative differences, figures (b) and (c) are qualitatively similar. The behaviour for other values of  $\epsilon$  is intermediate between those two.

In figures 5 (d), (e) and (f) we show steady-state rotations with angular frequency 1/2, as described in section 6.1. It is clear from the figures that the dependence on  $\epsilon$  and  $\alpha$  is rather weak. The lower bound (62) is violated in figures (d) and (f), so that a resonant steady state is not possible in those cases, but it is not violated in (e), which shows that steady states with angular velocity 1/2 and resonant ones can coexist. If we had chosen  $d\theta/d\tau(0)$  slightly different from 1 in figure (e), the solution we would have obtained numerically would have been a resonant one. In fact, finding these steady states numerically seems to require fine tuning of the initial conditions, that being the reason why we chose the same ones in the three figures.

## 7 Final remarks

In the foregoing sections we discussed several steady-state solutions to the equation of motion (4) with parametric excitation given by (3). We restricted our treatment to the parametrically excited rotator,

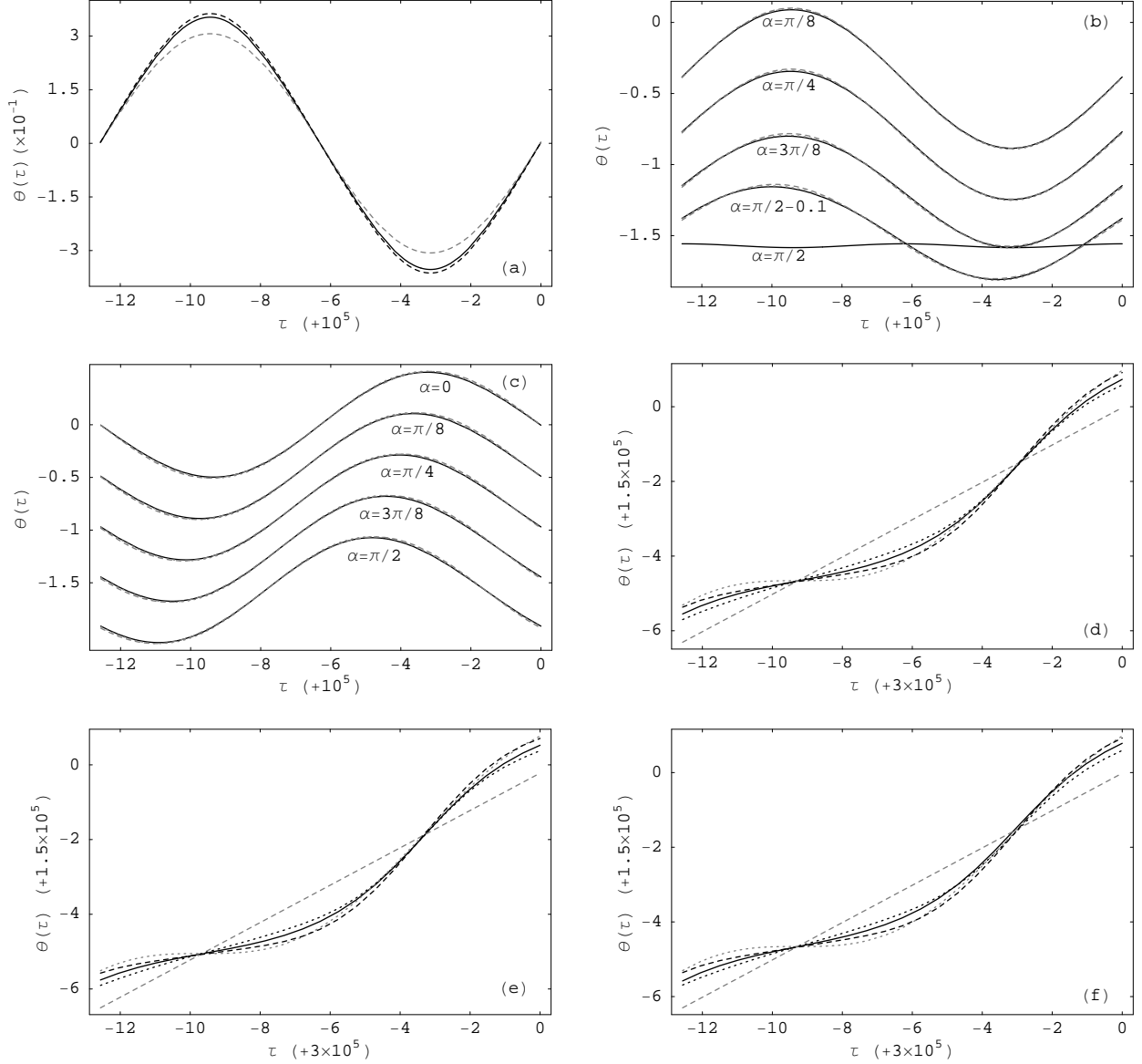


Figure 5: Solutions to equation (38) in the parametric-resonance region. Numerical solution (black solid line), compared with perturbative solutions at first (grey dashed line), second (grey dotted line) and third (black dashed line) orders as given in section 6. The parameters are set to (a)  $\epsilon = 0$ ,  $\alpha = 0$ ,  $n_{\varphi_1} = 0$ ,  $\Gamma = 0.203$ ,  $\Delta = 0.1$ ,  $\tilde{\lambda} = 5 \times 10^{-3}$ ,  $\theta(0) = 0$ ,  $d\theta/d\tau(0) = -10^{-4}$ ; (b)  $\epsilon = 0$ ,  $n_{\varphi_1} = 0$ ,  $\Gamma = 0.253$ ,  $\Delta = 0.01$ ,  $\tilde{\lambda} = 0.005$ ,  $\theta(0) = 0$ ,  $d\theta/d\tau(0) = 0.01$ ; (c)  $\epsilon = \pi/2$ ,  $n_{\varphi_1} = 1$ ,  $\Gamma = 0.253$ ,  $\Delta = 0.01$ ,  $\tilde{\lambda} = 0.005$ ,  $\theta(0) = 0$ ,  $d\theta/d\tau(0) = 0.1$ ; (d)  $\epsilon = 0$ ,  $\alpha = 0$ ,  $\Gamma = 0.243$ ,  $\Delta = 0.01$ ,  $\tilde{\lambda} = 5 \times 10^{-4}$ ,  $\theta(0) = 0$ ,  $d\theta/d\tau(0) = 1$ ; (e)  $\epsilon = 0$ ,  $\alpha = \pi/8$ ,  $\Gamma = 0.253$ ,  $\Delta = 0.01$ ,  $\tilde{\lambda} = 5 \times 10^{-4}$ ,  $\theta(0) = 0$ ,  $d\theta/d\tau(0) = 1$ ; (f)  $\epsilon = \pi/8$ ,  $\alpha = 0$ ,  $\Gamma = 0.244$ ,  $\Delta = 0.01$ ,  $\tilde{\lambda} = 5 \times 10^{-4}$ ,  $\theta(0) = 0$ ,  $d\theta/d\tau(0) = 1$ .

( $\Delta \lesssim 1$  in (4)), as opposed to the orbitally excited rotator ( $\Delta \gg 1$ ), and to low damping,  $10^{-5} \lesssim \tilde{\lambda} \lesssim 1$ . Similarly, for the pendulum we considered also  $\Gamma \lesssim 1$ . As mentioned in section 1, many other regimes are possible. Some of those may be treated as simple variants of the perturbative methods used here, as occurs, for example, with the two versions of the condition  $\Gamma \lesssim 1$  given in sections 5.2 ( $\Gamma = \mathcal{O}(\Delta)$ ) and 5.3 ( $\Gamma = \mathcal{O}(\Delta^3)$ ), which lead to slightly different perturbative expansions, with qualitatively different results. Yet, other parameter regions not considered here may require other mathematical tools. But even within the domain of parameter space considered here, and even within the class of simple steady states with  $\theta(\tau)$  either monotonic or periodic, our results are certainly not exhaustive.

In section 3 we discussed the linearly excited parametric rotator. We gave the necessary condition for steady-state rotations and showed that  $\theta(\tau) - \tau$  is a periodic function with period  $\pi$  that oscillates about a value  $\Theta$  determined by the parametric amplitude and the damping coefficient. There is also in that case a steady state in which the rotator oscillates about the transverse position. The latter solution seems to be unstable in the presence of gravity or eccentricity. In section 4 we extended those results to the case of elliptic motion of the suspension point. For steady-state rotations we generalised the results for linear excitation to any eccentricity, including circular excitation, for direct motion, and established the existence of contrarian steady state rotations for any elliptical excitation except the circular one. We treated also steady-state oscillations with the same angular frequency as the parametric excitation. Those oscillating steady-state solutions are characteristic of strictly elliptic excitation ( $0 < |\epsilon| < \pi/2$ ), since they do not exist for linear or circular motion of the suspension point. In the linear case the oscillating solutions reduce to equilibrium ones. The case of circular parametric excitation possesses some special characteristics that cannot be treated with the perturbative method discussed here, so we will discuss it separately [36].

In section 5 we considered the parametric pendulum. For steady-state rotations the perturbative theory with  $\Gamma \sim \Delta$  is only a slight modification of that with  $\Gamma = 0$  of section 4, with corrections due to gravity inducing odd angular frequencies in the spectrum of oscillations about uniform rotation. We obtained explicit expressions for those steady states, as functions of the eccentricity and angle with gravity. As in the case without gravity, contrarian-motion solutions exist for all  $\epsilon$  and  $\alpha$ , except for circular excitation. The steady-state oscillatory solutions with  $\Gamma \sim \Delta$  are very different from the case  $\Gamma = 0$ , because  $\Theta_0$  in that case is completely determined by gravity. By contrast, in the case  $\Gamma \ll \Delta$  the oscillating solutions are a small perturbation about the case  $\Gamma = 0$  and, in particular,  $\Theta_0$  is independent of gravity. This is the essential feature of the inverted-pendulum phenomenon: because  $\Gamma \ll \Delta$ , the dynamics are mainly determined by the torques of the inertial forces due to the motion of the suspension point, and not by those of gravity. We compute the angle  $\Theta$  about which these steady states oscillate as a function of the eccentricity of the suspension point's trajectory, as measured by the parameter  $\epsilon$ , and its angle  $\alpha$  with gravity. That result provides an analytical basis to the observation that, as a not-yet-inverted pendulum is slowly rotated from the downward to the upright position, it follows the motion of the parametric excitation with an angular lag [18]. More generally, as discussed in quantitative detail in that section and is intuitively expected, the dependence of the solutions to (4) on the angle  $\alpha$  between gravity and the major axis of the elliptic excitation is stronger for linear parametric excitation, and grows weaker as  $|\epsilon|$  is increased.

In section 6 we considered parametric resonance, for elliptic motion of the suspension point with arbitrary eccentricity and at an arbitrary angle  $\alpha$  with gravity. We found the explicit form of the oscillatory steady states in the resonance region, and their dependence with eccentricity and  $\alpha$ . Unlike the usually studied case of linear excitation parallel to gravity, when the excitation is not linear or not parallel to gravity, integer angular frequencies enter the spectrum of oscillations, besides the half-integer frequencies familiar from the case  $\epsilon = 0 = \alpha$ . We obtained necessary conditions for parametric resonance in terms of  $\epsilon$  and  $\alpha$ . In particular, for linear excitation the amplitude for parametric resonance vanishes at  $\alpha = \pi/2$ , but not for other eccentricities. We found also a steady-state rotation mode with angular frequency equal to half the parametric excitation frequency, in the parameter region associated with parametric resonance. Unlike the resonant solutions, however, the dependence of the steady-state rotations described in section 6.1 on the parametric excitation amplitude is analytic. Those rotation modes do not seem to have been discussed in the previous literature.

Finally, we want to stress that the steady states discussed above are only a handful out of a much more numerous spectrum. For linear and highly eccentric elliptic excitations there are other modes, even at small parametric excitation, that are of a rather different nature than those considered here and will be discussed separately. For circular and slightly eccentric elliptic excitations, as mentioned above, an extension of the methods presented here is necessary to uncover some of the simplest basic motions [36]. On the other hand,

for the steady states considered in this paper, the regions of stability and basins of attraction were probed rather crudely by means of numerical solutions to the equation of motion. More detailed and technically accurate analyses are required in those respects, which lie beyond the scope of the present paper and which we defer to future work.

## References

- [1] E. I. Butikov, “*On the dynamic stabilization of an inverted pendulum,*” Am. J. Phys. **69** (2001) 755–768.
- [2] E. I. Butikov, “*Subharmonic resonances of the parametrically driven pendulum,*” J. Phys. A **35** (2002) 6209–6231.
- [3] L. D. Landau, E. M. Lifshitz, “*Mechanics,*” Pergamon, 1976, 80–84.
- [4] V. I. Arnold, “*Mathematical methods of classical mechanics,*” Springer-Verlag, 1978, 113–120.
- [5] E. D. Yorke, “*Square-wave model for a pendulum with oscillating suspension,*” Am. J. Phys. **46** (1978) 285–288.
- [6] W. Case, “*Parametric instability: An elementary demonstration and discussion,*” Am. J. Phys. **48** (1980) 218–221.
- [7] I. Grosu, D. Ursu, “*Simple apparatus for obtaining parametric resonance,*” Am. J. Phys. **50** (1982) 325–328.
- [8] F. L. Curzon, A. L. H. Loke, M. E. Lefrançois, K. E. Novik, “*Parametric instability of a pendulum,*” Am. J. Phys. **63** (1995) 132–136.
- [9] T. E. Cayton, “*The laboratory spring-mass oscillator: an example of parametric instability,*” Am. J. Phys. **45** (1977) 723–732.
- [10] L. Falk, “*Student experiments on parametric resonance,*” Am. J. Phys. **47** (1979) 325–328.
- [11] B. A. Aničin, D. M. Davidović, V. M. Babović, “*On the linear theory of the elastic pendulum,*” Eur. Phys. J. **14** (1993) 132–135.
- [12] T. Yang, B. Fang, S. Li, W. Huang, “*Explicit analytical solution of a pendulum with periodically varying length,*” Eur. J. Phys. **31** (2010) 10891096.
- [13] E. I. Butikov, “*Parametric excitation of a linear oscillator,*” Eur. J. Phys. **25** (2004) 535–554.
- [14] E. I. Butikov, “*Parametric resonance in a linear oscillator at square-wave modulation,*” Eur. J. Phys. **26** (2005) 157–174.
- [15] D. R. Rowland, “*Parametric resonance and nonlinear string vibrations,*” Am. J. Phys. **72** (2004) 758–766.
- [16] R. Berthet, A. Petrosyan, B. Rõman, “*An analog experiment of the parametric instability,*” Am. J. Phys. **70** (2002) 744–749.
- [17] M. H. Friedman, J. E. Campana, L. Kelner, E. H. Seeliger, A. L. Yergey, “*The inverted pendulum: a mechanical analogy of the quadrupole mass filter,*” Am. J. Phys. **50** (1982) 924–931.
- [18] M. M. Michaelis, “*Stroboscopic study of the inverted pendulum,*” Am. J. Phys. **53** (1985) 1079–1083.
- [19] P. L. Kapitza, “*Collected Papers,*” D. Ter Haar editor, Pergamon, 1978, Vol. 2, 714–726.
- [20] L. D. Landau, E. M. Lifshitz, “*Mechanics,*” Pergamon, 1976, 93–95.
- [21] V. I. Arnold, “*Mathematical methods of classical mechanics,*” Springer-Verlag, 1978, 121–122.
- [22] D. J. Ness, “*Small oscillations of a stabilized inverted pendulum,*” Am. J. Phys. **35** (1967) 964–967.

- [23] H. J. T. Smith, J. A. Blackburn, “*Experimental study of an inverted pendulum,*” Am. J. Phys. **60** (1992) 909–911.
- [24] J. G. Fenn, D. A. Bayne, B. D. Sinclair, “*Experimental investigation of the “effective potential” of an inverted pendulum,*” Am. J. Phys. **66** (1998) 981–984.
- [25] F. M. Phelps, J. H. Hunter, “*An analytical solution of the inverted pendulum,*” Am. J. Phys. **33** (1965) 285–295; Am. J. Phys. **34** (1966) 533.
- [26] L. Blitzer, “*Inverted pendulum,*” Am. J. Phys. **33** (1965) 1076–1078.
- [27] H. P. Kalmus, “*The inverted pendulum,*” Am. J. Phys. **38** (1970) 874–878.
- [28] A. B. Pippard, “*The inverted pendulum,*” Eur. J. Phys. **8** (1987) 203–206.
- [29] J. A. Blackburn, H. J. T. Smith, N. Groenbech-Jensen, “*Stability and Hopf bifurcations in an inverted pendulum,*” Am. J. Phys. **60** (1992) 903–908.
- [30] D. J. Acheson, “*Multiple-nodding oscillations of a driven inverted pendulum,*” Proc. R. Soc. A **448** (1995) 8995.
- [31] W. T. Grandy, M. Schoeck, “*Simulations of nonlinear pivot-driven pendula,*” Am. J. Phys. **65** (1997) 376–381.
- [32] G. J. Mata, E. Pestana, “*Effective Hamiltonian and dynamic stability of the inverted pendulum,*” Eur. J. Phys. **25** (2004) 717–721.
- [33] L. Ruby, “*Applications of the Mathieu equation,*” Am. J. Phys. **64** (1996) 39–44.
- [34] S. Wolfram, “*The Mathematica Book,*” Third Edition, Cambridge U. Press, 1996.
- [35] J. Walker, “*The flying circus of physics,*” Wiley, 2006, 74.
- [36] A. O. Bouzas, “*The parametric rotator and pendulum with circular excitation,*” in preparation.

## A Parametric resonance with $\epsilon = 0 = \alpha$

In section 6 a solution  $\theta(\tau)$  at parametric resonance is given through  $\mathcal{O}(\Delta)$ . For  $\epsilon = 0 = \alpha$ , however, the terms of  $\mathcal{O}(\Delta)$  vanish, as explained in that section, so the correction at  $\mathcal{O}(\Delta^{3/2})$  becomes important. In this appendix we explicitly provide the coefficients  $A_3, B_3$  in (58) in that case.

When  $\epsilon = 0 = \alpha$ , consistency of the  $\mathcal{O}(\Delta^{5/2})$  equation for  $f_5(\tau)$  requires,

$$\begin{aligned}
 A_3 &= \frac{N_A}{D}, & B_3 &= \frac{N_B}{D}, \\
 N_A &= b_1 \cos \varphi_1 + a_1 \sin \varphi_1 + b_3 \cos(3\varphi_1) + a_3 \sin(3\varphi_1), \\
 b_1 &= -16h\rho_1(256 - 144\rho_1^2 - 256d\rho_1^2 + 3\rho_1^4), \\
 a_1 &= \rho_1(-2^{12} - 2^{13}d - 2^{11}\rho_1^2 - 2^9d\rho_1^2 + 2^{13}d^2\rho_1^2 + 192\rho_1^4 - 352d\rho_1^4 + 3\rho_1^6), \\
 b_3 &= 768h\rho_1^3, & a_3 &= 48\rho_1^3(16 + 32d + \rho_1^2), \\
 N_B &= b'_1 \cos \varphi_1 + a'_1 \sin \varphi_1 + b'_3 \cos(3\varphi_1) + a'_3 \sin(3\varphi_1), \\
 b'_1 &= \rho_1(2^{12} - 2^{13}d - 2^{11}\rho_1^2 + 2^9d\rho_1^2 + 2^{13}d^2\rho_1^2 - 192\rho_1^4 - 352d\rho_1^4 + 3\rho_1^6), \\
 a'_1 &= 16h\rho_1(256 + 144\rho_1^2 - 256d\rho_1^2 + 3\rho_1^4), \\
 b'_3 &= 48\rho_1^3(-16 + 32d + \rho_1^2), & a'_3 &= -768h\rho_1^3, \\
 D &= 64(-2^8 + 2^{10}d^2 + 2^8h^2 - 2^7d\rho_1^2 + 3\rho_1^4 + 32\rho_1^2 \cos(2\varphi_1)),
 \end{aligned}$$

with  $\rho_1, \varphi_1$  as defined in (57), and with  $h = \tilde{\lambda}/\Delta, d = \delta/\Delta$ .